INTERIM REPORT

ACOUSTIC EMISSION MONITORING OF STEEL BRIDGE MEMBERS

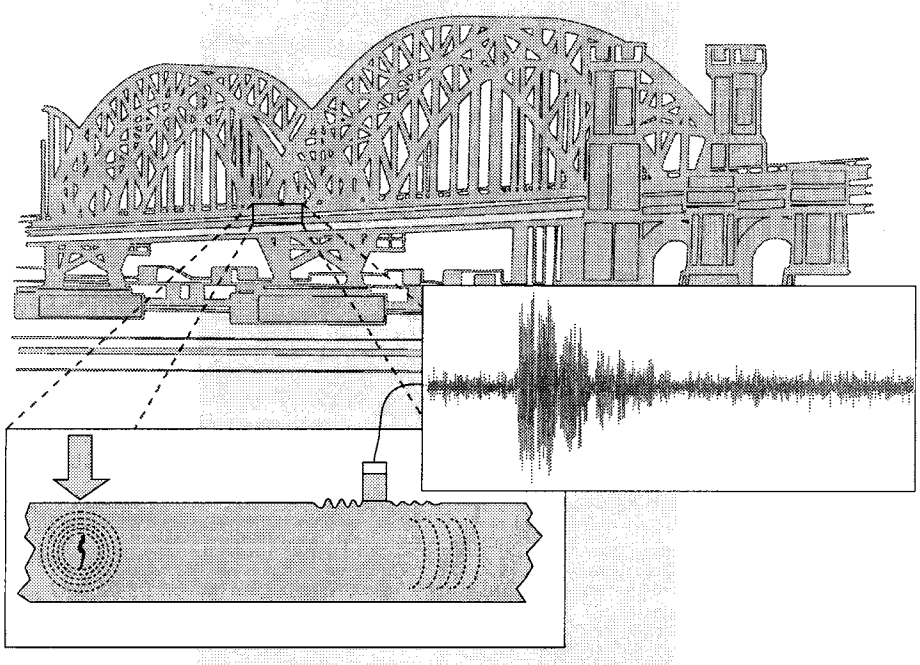

GERARDO G. CLEMEÑA, Ph.D.
Principal Research Scientist

MARGARIT G. LOZEV, Ph.D.
Research Scientist

JOHN C. DUKE, Jr., Ph.D.
Professor

MIGUEL F. SISON, Jr.
Graduate Research Assistant

V · I · R · G · I · N · I · A
VTRC
TRANSPORTATION RESEARCH COUNCIL

VIRGINIA TRANSPORTATION RESEARCH COUNCIL

Technical Report Documentation Page

1. Report No.	2. Government Accession No.	3. Recipient's Catalog No.
FHWA/VTRC 95-IR1		

4. Title and Subtitle	5. Report Date
Interim Report: Acoustic Emission Monitoring of Steel Bridge Members	May 1995
	6. Performing Organization Code
7. Author(s)	8. Performing Organization Report No.
G. G. Clemeña, M. G. Lozev, J. C. Duke Jr., and M. F. Sison Jr.	VTRC 95-IR1
	10. Work Unit No. (TRAIS)
9. Performing Organization Name and Address	
Virginia Transportation Research Council 530 Edgemont Road Charlottesville, Virginia 23219	11. Contract or Grant No. 3069-010
	13. Type of Report and Period Covered
12. Sponsoring Agency Name and Address	Interim Report
Virginia Department of Transportation 1401 E. Broad Street Richmond, Virginia 23219	14. Sponsoring Agency Code

15. Supplementary Notes

In cooperation with the U.S. Department of Transportation, Federal Highway Administration.

16. Abstract

This interim report describes the current status of acoustic emission (AE) monitoring of steel bridge members. The report includes a brief introduction to the theory of acoustic emission and a comprehensive summary of previous efforts to apply AE monitoring to steel bridges, and discusses issues related to AE noise discrimination.

Five bridges were field tested. Extensive data from the active cracking of a hanger on the Rte. 29 bridge over the Robinson River at Madison, Virginia, are discussed. The report includes conclusions and recommendations based on extensive field monitoring. Two appendices detail the laboratory fatigue testing of bridge steels and the simulated environmental exposure of AE transducer-mounting adhesives.

AE monitoring is sensitive to the acoustic energy emitted by steel bridge members during the formation and growth of cracks. It is the only method that can distinguish between active and benign cracks. It is also possible to discriminate between AE caused by crack growth and irrelevant noise. AE information can be significant in making repair or replacement decisions, and AE could be used for the continuous remote monitoring of critical bridge members or even entire bridges.

17. Key Words	18. Distribution Statement
Acoustic emission, monitoring, steel, bridge, noise, cracks	No restrictions. This document is available to the public through NTIS, Springfield, VA 22161.

19. Security Classif. (of this report)	20. Security Classif. (of this page)	21. No. of Pages	22. Price
Unclassified	Unclassified	68	

INTERIM REPORT

ACOUSTIC EMISSION MONITORING OF STEEL BRIDGE MEMBERS

Gerardo G. Clemeña, Ph.D.
Principal Research Scientist

Margarit G. Lozev, Ph.D.
Research Scientist

John C. Duke, Jr., Ph.D.
Professor

and

Miguel F. Sison, Jr.
Graduate Research Assistant

Virginia Transportation Research Council
(A Cooperative Organization Sponsored Jointly by the
Virginia Department of Transportation and the University of Virginia)

In Cooperation with the U.S. Department of Transportation
Federal Highway Administration

Charlottesville, Virginia

May 1995
VTRC 95-IR1

Bridge Research Advisory Committee

C. A. Nash, Chairman, District Administrator-Suffolk, VDOT
J. P. Gomez, Executive Secretary, Research Scientist, VTRC
G. W. Boykin, District Materials Engineer-Suffolk, VDOT
N. W. Dillon, District Structure & Bridge Engineer-Salem, VDOT
P. Hoadley, Associate Professor, Department of Civil Engineering, VMI
M. T. Kerley, Structure & Bridge Division Administrator, VDOT
T. F. Lester, Structure & Bridge Division, VDOT
L. L. Misenheimer, District Structures and Bridge Engineer-Staunton, VDOT
C. Napier, Structural Engineer, Federal Highway Administration
W. L. Sellars, District Structures and Bridge Engineer-Lynchburg, VDOT
D. B. Sprinkel, District Structure and Bridge Engineer-Culpeper, VDOT
J. F. J. Volgyi, Jr., Transportation Engineer Program Supervisor, Structure & Bridge Division, VDOT
R. E. Weyers, Professor of Civil Engineering, VPI & SU

ABSTRACT

This interim report describes the current status of acoustic emission (AE) monitoring of steel bridge members. The report includes a brief introduction to the theory of acoustic emission and a comprehensive summary of previous efforts to apply AE monitoring to steel bridges, and discusses issues related to AE noise discrimination.

Five bridges were field tested. Extensive data from the active cracking of a hanger on the Rte. 29 bridge over the Robinson River at Madison, Virginia, are discussed. The report includes conclusions and recommendations based on extensive field monitoring. Two appendices detail the laboratory fatigue testing of bridge steels and the simulated environmental exposure of AE transducer-mounting adhesives.

AE monitoring is sensitive to the acoustic energy emitted by steel bridge members during the formation and growth of cracks. It is the only method that can distinguish between active and benign cracks. It is also possible to discriminate between AE caused by crack growth and irrelevant noise. AE information can be significant in making repair or replacement decisions, and AE could be used for the continuous remote monitoring of critical bridge members or even entire bridges.

TABLE OF CONTENTS

ACOUSTIC EMISSION MONITORING OF STEEL BRIDGE MEMBERS

Gerardo G. Clemeña, Ph.D, Principal Research Scientist,
Margarit G. Lozev, Ph.D., Research Scientist,
John C. Duke, Jr., Ph.D., Professor, and
Miguel F. Sison, Jr., Graduate Research Assistant

INTRODUCTION

Bridges must be protected against unanticipated failure in service, in the interests of public safety and investment. Continued improvements in civil and structural design and the development of better construction materials have improved the durability of bridges. However, a significant number of aging bridges have been subjected to cyclic loads above the number for which they were designed. Corrosion loss remains the biggest cause of deterioration in steel bridges, but the few recorded failures have been due to fatigue crack growth. Bridge engineers need fail-safe inspection and evaluation tools and procedures to detect crack growth at an early stage and monitor it effectively. This is especially crucial for bridges with fracture-critical members, whose failure would endanger the safety of motorists.

Most bridge inspection is done by visually examining the entire structure, emphasizing sections and details that, in the inspector's experience and judgment, are prone to developing defects. This method depends greatly on the ability and motivation of the inspector. Visual methods are supplemented by nondestructive evaluation (NDE) techniques that may include magnetic particles, dye penetrants, eddy current, ultrasound, and x-ray radiography. The choice of methods depends on the type of material, construction details, accessibility of the defect, and overall cost. These techniques have been very useful despite their limitations, which include problems in detecting small cracks, the mostly operator-dependent interpretation of results, the operator's need for close access to the part being tested, and the sometimes high associated costs. However, none of these NDE techniques is suitable for monitoring.

Acoustic emission (AE) monitoring, which is sensitive to the acoustic energy emitted by a steel member during the formation and growth of cracks, offers a promising alternative. It is the only method that can distinguish between active and benign cracks. Such information can be significant in making repair or replacement decisions. In addition, AE could be used for the continuous remote monitoring of critical bridge members or even entire bridges. Structures made of other materials, such as reinforced concrete, masonry, wood, and aluminum may also be monitored by AE, although at present few studies of such applications exist.

This interim report presents the results of an ongoing project to develop practical field knowledge and techniques for monitoring acoustic emission from steel bridge members. It details the methods and findings from the actual monitoring of several bridges in Virginia and the laboratory work done in support of the field tests, emphasizing the procedures and analysis used to discriminate between AE produced by crack growth and irrelevant noise.

PROBLEM STATEMENT

Past studies of AE have not fully developed the engineering application of AE to bridge monitoring. In particular, unwanted noises associated with bolt fretting and rubbing or traffic must be distinguished systematically from sounds associated with crack initiation or growth, to monitor critical regions of a structure reliably.

PURPOSE AND SCOPE

The objectives of this study were (1) to study and characterize the AE associated with various sources of noise in a typical bridge environment, and (2) to develop relevant expertise in the Virginia Department of Transportation consistent with guidelines on AE soon to be released by the Federal Highway Administration.

THEORY OF ACOUSTIC EMISSION

Acoustic emission from a growing defect in steel or other metals is generally associated with plastic deformation around the crack tip and the fracture of inclusions along the path of the growing crack, among other things. The damage rapidly releases strain energy, part of which is converted to stress waves propagating inside or on the surface of the metal. Sensors acoustically coupled to the surface can detect the disturbance. These sensors, the most common of which have active elements made from a piezoelectric material, convert the detected surface mechanical oscillation into electrical voltage. The electronic circuitry of a data acquisition instrument then measures the acoustic emission parameters from the detected signal.

Figure 1 shows a typical AE signal, with the corresponding time-domain parameters labeled accordingly. This method of characterizing AE is called the ringdown technique. The values of most of the measured parameters depend on the choice of threshold level. The preset threshold level determines in part the sensitivity of the AE system, and its selection is based on the strength of the signals targeted for measurement and the level of background noise. Another way to characterize an AE event involves capturing a digitized waveform of the signal and extracting frequency-domain characteristics.

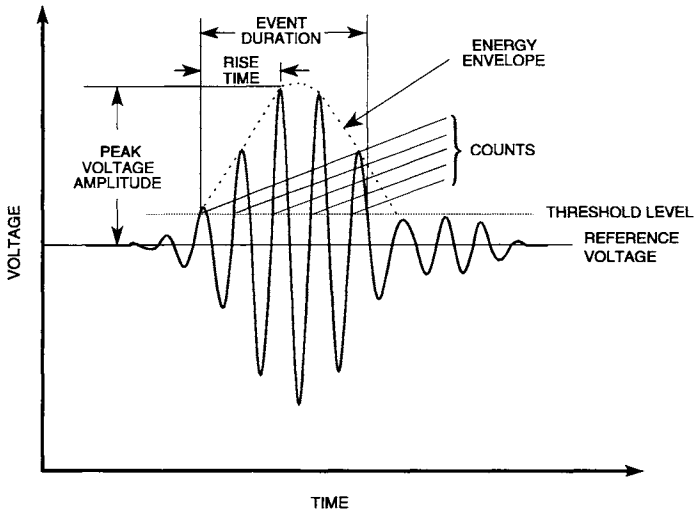

Figure 1. Typical AE signal, with time-domain parameters

Ideally, the AE method is significantly more sensitive than other NDE methods in detecting crack presence. However, any disturbance of the test piece, mechanical, electrical or hydraulic, can produce detectable acoustic signals. The main limitation on the field application of AE for monitoring structures is that numerous sources of noise complicate the detection of defect-related AE. On steel bridges, possible sources of noise include traffic, oxide fracture, paint decohesion, fretting from various surfaces rubbing against each other, and precipitation. Even the defect itself generates irrelevant signals, such as crack face rubbing.

HISTORICAL BACKGROUND

Basic research has been conducted on acoustic emission since instrumented testing was first reported in 1936. The engineering application of this NDE method to testing steel bridges has been studied for over 20 years.

In 1971, Pollock and Smith collected AE data during proof testing of a portable tank bridge for the British Ministry of Defense.[1] They demonstrated that AE signals recorded in the field could be associated with test results on laboratory specimens. In 1972, scientists from the Argonne National Laboratory monitored AE from a bridge on Interstate 80 in Illinois.[2] In 1973 Hopwood monitored AE from eyebar members of a bridge and found good transmission through eyebar members, although noise was also found to be a serious problem.[3]

An extensive FHWA/Battelle Pacific Northwest program in the late 1970's developed a battery-powered digital acoustic emission monitor (DAEM).[4,5] This device allowed AE data to be stored on erasable programmable read-only memory (EPROM) chips for additional processing and evaluation upon periodic collection. The study demonstrated the utility of fre-

quency spectrum analysis and the potential for centralized signal processing. Again, the AE associated with bridge component damage was accompanied by AE signals related to noise.

From August 1980 to July 1982, the Kentucky Transportation Research Center used DAEM to monitor a bridge on Interstate 471, identifying traffic and rainfall as sources of AE noise.[6] In the early 1980's, the Dunegan Corporation, under contract from the West Virginia Department of Highways, examined the practical difficulties of long-term AE bridge monitoring.[7] The cost benefits of AE monitoring compared to periodic ultrasonic, magnetic particle or liquid penetrant inspection of known defects were discussed.

Miller et al. of United Technologies Research Center, under contract from FHWA, used laboratory and field tests to characterize AE signals from flaws and various noise-related AE sources.[8] They explored different approaches using both time and frequency domain representations of AE signals. The use of pattern recognition and source classification for filtering out noise AE and for discriminating between different damage-related AE events like brittle fracture and fatigue was demonstrated. A field-worthy AE sensor, able to detect a broad band of frequencies, was developed during the program.

Prine and Hopwood considered an AE weld monitoring (AEWM) system for both fabrication and in-service evaluations of bridge components.[9] They pointed out that AE from bridges depends on traffic volume and vehicle speed and weight, as well as structural details and transducer characteristics.

In 1987, Vannoy et al. of the University of Maryland monitored the Woodrow Wilson Bridge between Maryland and Virginia for the Maryland Department of Transportation. They found that the predominant peak frequency of noise AE is distinctly lower than crack-related AE.[10] Suitable software filters, designed to exclude AE whose time domain parameters do not fall within the range of parameters of crack-related AE, eliminated most noise signals. In 1991, the same group conducted extensive laboratory tests on full-size A588 bridge beams.[11] The AE parameters of cracks versus noise on rolled, welded and cover-plated beams were characterized in both time and frequency domains. It was also determined that corrosion has no effect on the time domain parameters of AE from cracks. In a related study, Hariri of the University of Maryland sought to develop a database of signal characteristics from different bridge steels, various material and loading conditions, and different part geometries and thicknesses for use in bridge structure AE testing.[12] Noise filters can be developed using ranges of AE parameters dictated by the type of material, thickness, paint layer and corrosion conditions of a monitored part. The surface paint layer did not attenuate AE signals significantly.

The Physical Acoustics Corporation field-tested several bridges for the FHWA. Various bridge details required source location and guard sensors for filtering out irrelevant AE events.[13,14,15] AE was used for testing the effectiveness of retrofits as well as finding new cracks.

In Canada, Gong et al. used AE to monitor 36 railroad bridges for the Canadian National Railways over a period of three years.[16] Using a known functional relationship between AE count rate and the stress intensity factor range, they classified cracks into 5 levels of severity. Spatial discrimination and filtering eliminated noise by using AE parameter windows determined from laboratory tests on bridge steels.

In 1993, Prine further demonstrated the effectiveness of combining AE and strain gage monitoring on three bridges in Wisconsin and California.[17] In a departure from the usual crack characterization function of AE monitoring, a bascule bridge was tested to determine the cause of loud impact noises that accompanied the lifting and lowering of the bridge.

Overall, research has provided a reasonable scientific base for using AE in a bridge management program. Continued advances in electronics, such as faster microprocessors, provide testing capabilities that were not possible just a few years ago. Since AE relies heavily on instrumentation, better results will be obtained with improved electronics.

NOISE DISCRIMINATION IN AE TESTING

This study explored three methods of separating unwanted noise from relevant AE: spatial discrimination, load discrimination, and signal discrimination.

Spatial discrimination is possible because AE techniques can locate emission sources. Source location is calculated from the time differences in the arrival of emission event signals at two or more carefully positioned sensors. Possible sensor configurations include linear, triangular, rectangular, and 3-dimensional placements. The source must be located be within the area or line bounded by the locating sensor array, to effectively filter out noise sources outside the crack monitoring array. The success of this method depends on how far the noise source is from the defect, the sensitivity and accuracy of the source location function of the AE instrumentation, and the space available for transducer placement. Multiple wave paths on the monitored part can cause erroneous source location results, which can be corrected by using guard sensors for zone isolation. These sensors are positioned so that any emission event originating outside the area of interest would arrive at these sensors first. Knowing the location of possible noise sources would greatly enhance the effectiveness of guard sensors.

Load or parametric discrimination is usually done with a strain-measuring device. Since flaw growth is only expected when the member being monitored is stressed beyond a certain level, AE detected at levels below this can be filtered out as noise. This method is particularly effective in distinguishing between AE from actual flaw growth and AE produced by the interaction of crack faces during compression (including possible AE produced by the crushing of corrosion products between crack faces in environmentally exposed defects).

Signal discrimination is a broad term for techniques that use peculiarities in the features of AE signals from different sources. These features are a function of several variables, including the nature (or rate of energy release) of the AE source, the material and geometry of the structure through which the AE waves propagate, the sensor resonant properties, and the distance from source to sensor.

If the range of a time domain parameter of AE from crack growth, such as amplitude, can be established, filters can be devised to exclude all detected signals that do not fall within this range. More effective filtering is achieved as more parameters are included. Some AE data acquisition systems have such methods of filtering as standard features. For example, AE from cracks are known to have short risetimes compared to the signal duration. It would thus be a simple step to eliminate noises that have long risetimes.

Features from the frequency domain can likewise be used to distinguish noise. Most mechanical noises, like those generated by machinery, have frequencies of less than 50 KHz. AE from crack-growth in metals has been shown to be wideband. A sensor whose resonant frequency is higher than that of noise will not receive such noise signals. Full frequency analysis can be used to eliminate further noise, such as fretting, with frequency domain properties less evidently different from crack emission.

A more involved signal characterization method uses statistical pattern recognition techniques to classify AE from different sources. A reduced set of features, derived from a larger set that may include time and frequency domain characteristics as well as other quantifiable information regarding the AE event, is chosen based on the ability to classify events from different sources into their correct sets. Computer algorithms that automatically classify AE events are then developed.

METHODS

Instrumentation

Acoustic Emission Data Acquisition System

An 8-channel Spartan AT AE data acquisition system manufactured by PAC was used to test the bridges. The entire system consisted of the Spartan unit and a 386 MHz personal computer (PC) (Figure 2). All system functions were controlled by the SA-LOC software program running in a DOS environment. Figure 3 is a block diagram of the system.

Figure 2. Spartan unit and 386 MHz personal computer.

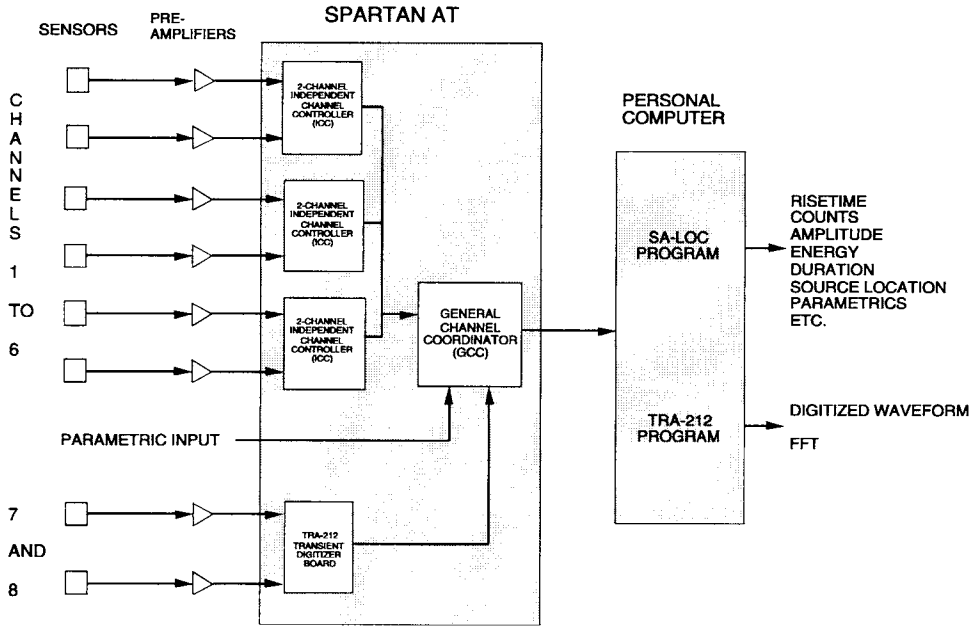

Figure 3. Block diagram of Spartan AT AE data acquisition system.

Six of the 8 channels available were used for signal measurement. These contained the circuitry outputting the time domain parameters of an AE event -- counts, risetime, energy, peak amplitude, RMS and duration. The two remaining channels digitized and stored AE waveforms using the PAC TRA-212 Transient Recorder Analyzer system. The Spartan also had up to four parametric inputs, which were used to record load data in the laboratory tests and strain gage output in the bridge tests.

SA-LOC was a menu-driven program that set up the Spartan hardware unit and was capable of real time display and post test graphical replay of data. This last feature was a powerful data analysis tool enabling the user to display plots of the various measured signal parameters, parametric values and source location results in more than 150 combinations.

Filters could be set up with the SA-LOC to accept or reject signals before the main processor board was reached. Up to four filters of user-chosen AE parameters could be configured. Only signals falling between the low and high levels specified for each parameter were processed and stored as data.

The source location function of the Spartan system was configured in the location set-up menu of the SA-LOC. Four different types of source location algorithms were available: zonal, linear, triangular and rectangular. In zonal source location, an AE event was assigned to the location of the first transducer that detected it. This was most useful in implementing guard sensors. Most of the tests performed were configured for both zonal and linear location.

The TRA-212 had a maximum digitization rate of 10 MHz and was capable of storing up to 2 Mb length samples in memory. The software controlled the digitizing boards, recorded and stored the measured data on disks, and performed various display and analysis functions. The frequency spectra of signals were calculated using the Fast Fourier Transform (FFT) algorithm and could be displayed in real time or during post-test analysis. Three modes of triggering were available, of which external threshold triggering was used in all the tests. Signal voltages of up to 10 V could be recorded and a maximum threshold sensitivity of 0.01 V was attainable.

TRA-212 could be run either separately or simultaneously with SA-LOC. The latter was accomplished by running TRA in background mode while data acquisition was performed with SA-LOC. This was particularly useful during the bridge tests, since SA-LOC supplied the source location and strain gage data needed to classify the different AE waveforms recorded by TRA-212.

Sensors and Auxiliary Equipment

Two types of piezoelectric transducers, the R30I and the WD, both manufactured by PAC, were used (Figure 4). The R30I, a resonant transducer with a peak resonant frequency of approximately 350 KHz, had an integral preamplifier with a gain of 40 dB. The WD, a wide-band transducer with a relatively flat frequency response between 100 KHz and 1 MHz, was a differential transducer requiring a separate external preamplifier. A PAC model 1220A preamplifier with a highpass frequency filter of 20 KHz was used.

Magnetic hold-downs attached the R30I sensors to the parts to be monitored. Strips of duct tape or a cyanoacrylate adhesive were used to mount the WD sensors. Except where the adhesive was used, a thin layer of vacuum grease couplant was applied on the interface between the transducer and the part surface to aid in the transmission of AE signals.

The strain gage used was a Micro Measurements Precision type EA-O6-20CBW-120 (Measurements Group, Inc.), a general purpose gage designed for strain averaging measurement on large specimens. It had a matrix length of 62.4 mm (2.46 ") and a width of 8.12 mm (0.32 "). The gage was attached using M-Bond 200, a methyl-2 cyanoacrylate adhesive.

Shielded RG50 coaxial cables, 15.24 m (50 feet) in length, connected the sensors (or the pre-amp of the WD sensor) to the Spartan unit. A portion of each cable close to the sensors was either looped around or taped to a secure part of the bridge to prevent the weight of the cable from pulling on the sensors and affecting the quality of the acoustic coupling between sensor and part surface.

A portable gasoline-fueled generator powered all instrumentation. Except for the need to periodically shut down the system for refueling, there was no problem with the power source.

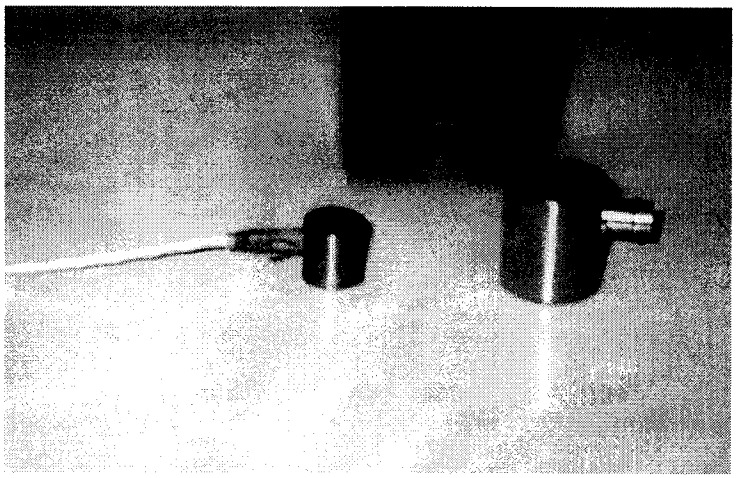

Figure 4. R30I and WD piezoelectric transducers with R30I magnetic holddown.

Bridge Testing Set-Up Procedure

Procedures common to all the bridge tests, mainly the steps taken to ensure that valid AE data were detected and stored, are discussed below.

With all sensors in place, the traditional pencil lead break test was performed for each sensor and source location sensor array. This test consisted of breaking a 0.5 mm-diameter pencil lead approximately 1.5 mm from its tip by pressing it against the surface of the piece. This generated an intense acoustic signal that was detected by the sensors as a strong burst of AE. The purpose of this test was twofold. First, it ensured that the transducers were in good acoustic contact with the part monitored. Generally, the breaks should register amplitudes of at least 80 dB for a reference voltage of 1 mV and a total system gain of 80 dB. Secondly, it checked the accuracy of the source location setup, indirectly determining the actual value of the acoustic wavespeed.

The SA-LOC software required the user to enter a value for the acoustic wavespeed of the material being tested. In acoustic emission testing, this could be anywhere between the velocity of longitudinal bulk waves and that of surface waves. The effective wavespeed, however, could vary from test to test, influenced by the geometry and condition of the part being tested. An approximate value of this wavespeed was determined using the differences in the time of arrival of lead break signals at two separate transducers.

With the actual wavespeed entered into the computer, further lead break tests checked the source location accuracy. The lead was broken close to the area of interest, which in most tests was the tip of a known crack, while the location of the detected signal on an event-position graph was checked. A consistently correct location reading indicated the sensors were ready. It should be noted that source location algorithms were implemented completely in software. Location results could be fine-tuned during post-test analysis by using different wavespeed values or different sensor configurations, such as those with guard sensors, without changing the original data or sacrificing information during data collection.

Setting the threshold levels of both the SA-LOC and the TRA was the final step. Maximum sensitivity was always desired, but the choice was constrained by the level of background noise. A practical and obvious basis for the optimum threshold level was that no AE should be detected when no vehicles were passing over the bridge. Except as noted, a gain of 40 dB and a floating threshold of 25 dB were used with the SA-LOC; the preamps provided a nominal 40 dB of gain as well.

RESULTS AND DISCUSSION

Case 1: New River Bridge

AE monitoring was performed on the Rte. 460 west-bound bridge over the New River in Glenlyn, VA on September 24, 1993. The bridge was a continuous span, multi-girder bridge with 16 pin-and-hanger and 8 pin-and-hinge connections. Since 1990, suspected cracks in four pins have been monitored using ultrasonic inspection. It was decided to replace all the pins and hangers, which are of A588 weathering steel, with A276 stainless steel material. VDOT contractors were in the process of replacing the pins when the test was conducted.

Two pin-and-hanger connections on the western end of the west-bound lanes were chosen for monitoring. One had a crack; the other was newly installed. The monitoring equipment was positioned under the bridge close to the pins, about 4.6 m (15 ft) above the ground.

The pins were 0.31 m (1 ft) long and 102 mm (4 in) in diameter at the widest section. An R30I sensor was attached to each end of the two pins, as close as possible to the axial center of the pin. Figure 5 shows one end of a cracked pin where a sensor was placed. Magnetic hold-downs attached the sensors to the cracked pin, while duct tape was used to mount the sensors on the stainless steel pin. The Spartan system was configured to perform linear source location and an old pin that had been removed before the test was used to check the accuracy of the system settings. Since the pins being monitored were not exposed, the actual sensor set-up was simulated on the old pin and pencil lead break tests were performed along the length of this pin.

Figure 5. Pin and hanger connection, Rte. 460 bridge in Glenlyn, VA. Sensor and magnetic hold-down are attached to the end of the pin.

The live loading of the bridge was exclusively the normal passing traffic, although one lane (passing lane) was closed for repair work. Data was collected for 1 hour and 52 minutes at the old pin. The new pin was monitored for 18 minutes. Source location results for the cracked pin and the new pin are plotted in Figure 6. The boxed numbers below the x-axis indicate the position and number designation of the sensors. Sensors 1 and 2 were attached to the cracked pin. The new pin had sensors 3 and 4.

Ultrasonic inspection had indicated a crack 102 mm (4 ") from sensor 1. However, there was no obvious clustering of events at this location, which would have been a good indication of an active crack. Differences in the AE characteristics of events occurring between 0.91 and 127 mm (3 " to 5 ") and the other detected AE events (which were presumed to be rubbing noise) were investigated. The ranges of signal characteristics (counts, amplitude, etc.) of the two groups completely overlapped.

Using the acoustic emission method to monitor pins and similar fasteners presents a special challenge. The presence of fretting noise sources close to or at the defects prevents the use of spatial discrimination to distinguish flaw-related AE signals from noise. Other means of discrimination must be employed. Possibly the waveform and frequency analysis of AE signals may prove useful for pin-and-hanger components.

The newly installed stainless steel pin was monitored for a different purpose. It has been postulated that the seizing of pins due to corrosion contributes to crack growth, since this produces added torsion and bending loads not necessarily accounted for in the design of the pins. Possibly the AE sensors will detect the rubbing of a freely rotating pin against the mating pin and hanger surfaces, thus determining qualitatively if a pin is seized or not.

Figure 6 shows events for the new pin that were detected over an 18-minute period. A total of 125 events occurred between the ends. In comparison, the cracked pin was monitored for close to two hours, and showed only 114 events. It is natural to expect limited movement from the old pin, and this is shown by the results. However, the greater event rate for the new pin could be due to mating surfaces not yet smoothed by constant rubbing.

The use of AE in this manner should be approached with caution as it is entirely qualitative. The results from a particular pin should be compared to another similarly configured pin known to be moving freely in order to gauge the extent of seizing.

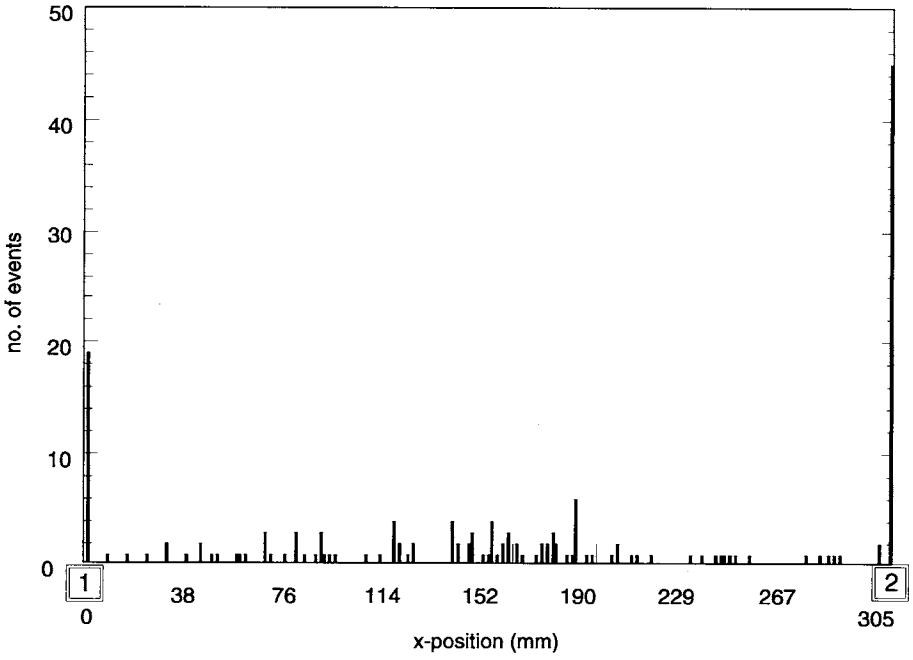

Figure 6A. Source location results for cracked pin, showing no evident crack activity.

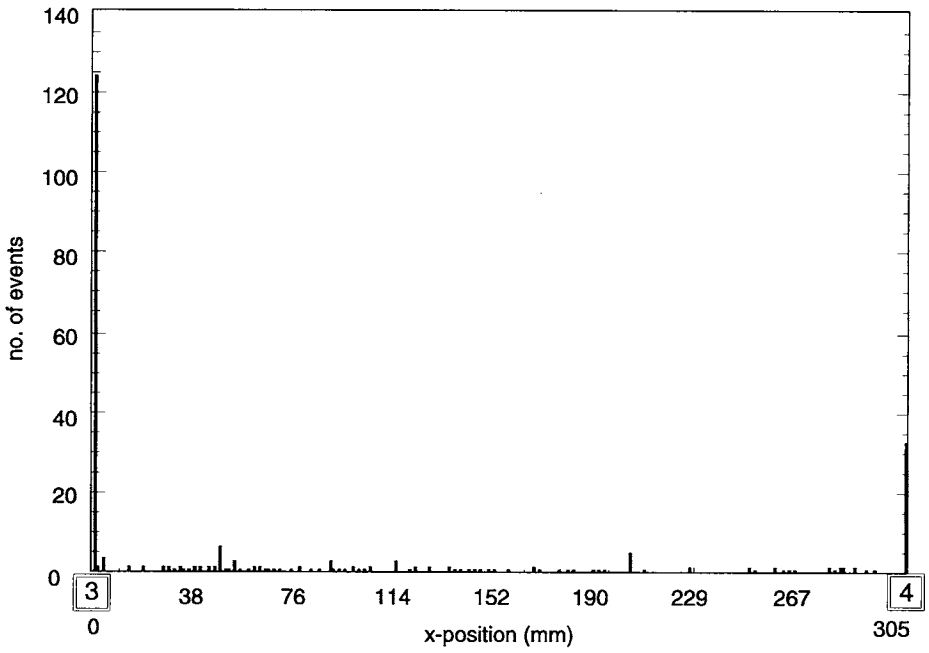

Figure 6B. Source location results for new pin.

Case 2: Staunton River Bridge

The Rte. 29 bridge over the Staunton River in Altavista, VA was monitored on July 19, 1994. VDOT personnel who helped perform the tests suggested the locations to be monitored. Two sites, accessed using the Bridgemaster, were chosen for monitoring. Figure 7 shows the bridge, with an outer girder similar to the one monitored.

The first location was on the 9.5 mm (3/8 ") thick cracked web of an inner girder retrofitted with a 9.5 mm (3/8 ") thick splice plate bolted to the web (Figure 8). The crack continued to grow in spite of the retrofit, and had progressed past the splice plate and under the bolted angular connector to the diaphragm. R30I sensors 1 and 2, spaced 155 mm (6 1/2 ") apart, were set up for linear source location to detect activity at the lower exposed end of the crack. A third sensor was attached to the flange as a guard sensor to distinguish fretting noise from the flange bolts.

The second location was on the same cracked girder. Holes had been drilled at both ends of the crack to arrest further growth. R30I sensors 3, 4 and 5 were positioned for triangular planar source location (Figure 9) to detect crack activity past the lower stop drill hole, which was right above the flange weld.

The Spartan unit and the PC were set up above the bridge, leaving only the inner lane open to traffic. Loading was accomplished via normal bridge traffic. The first location was monitored for approximately one hour, and the second location for about 45 minutes.

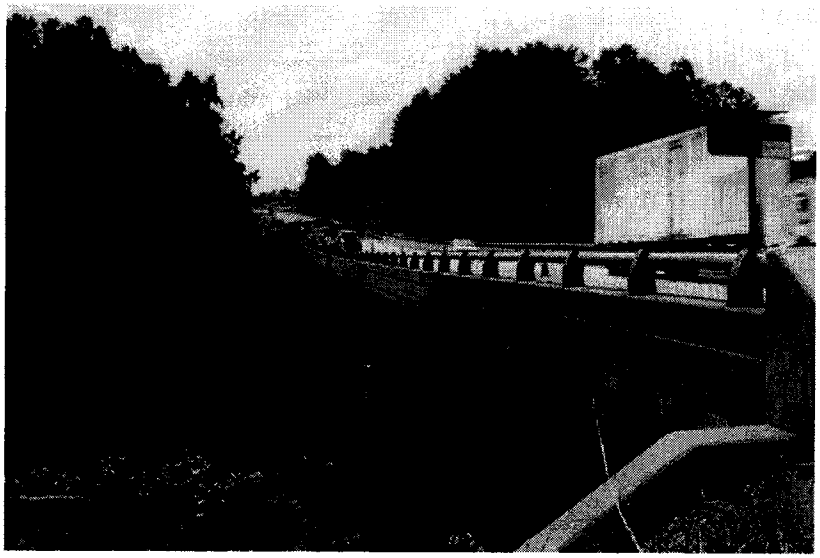

Figure 7. Rte. 29 northbound bridge over the Staunton River, Altavista, VA.

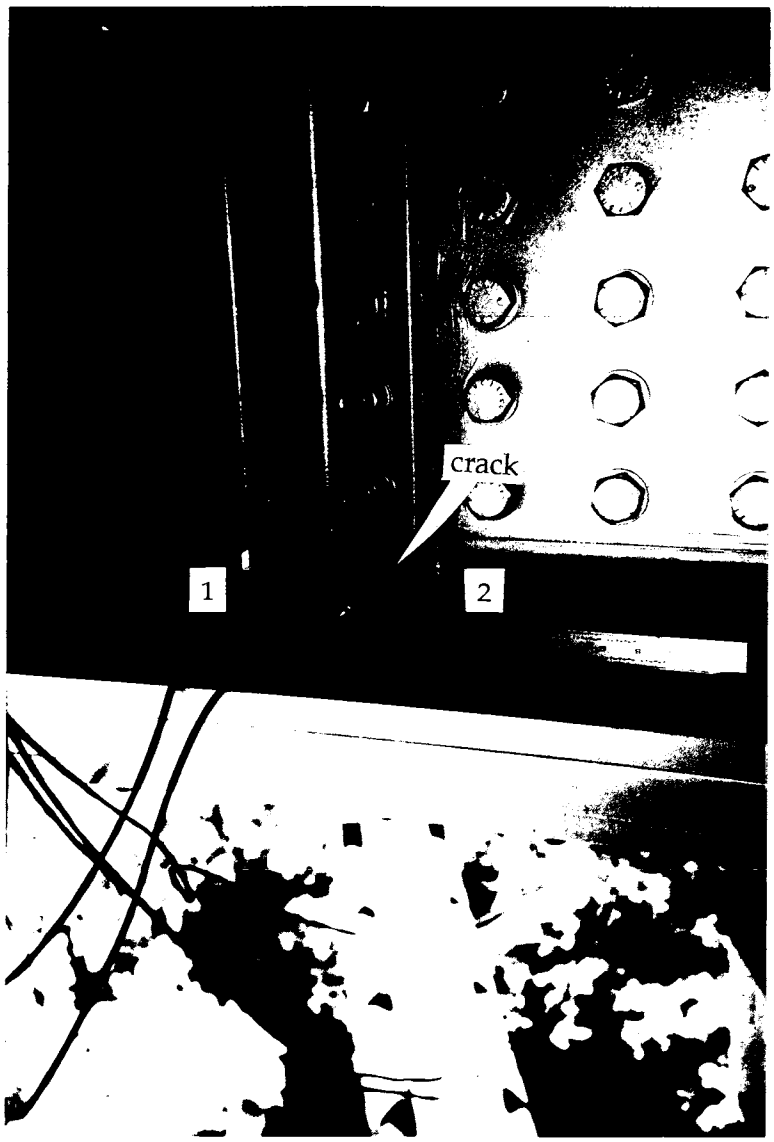

Figure 8. View of sensor placement at location 1 showing sensors 1 and 2, positioned for linear source location, and guard sensor 3.

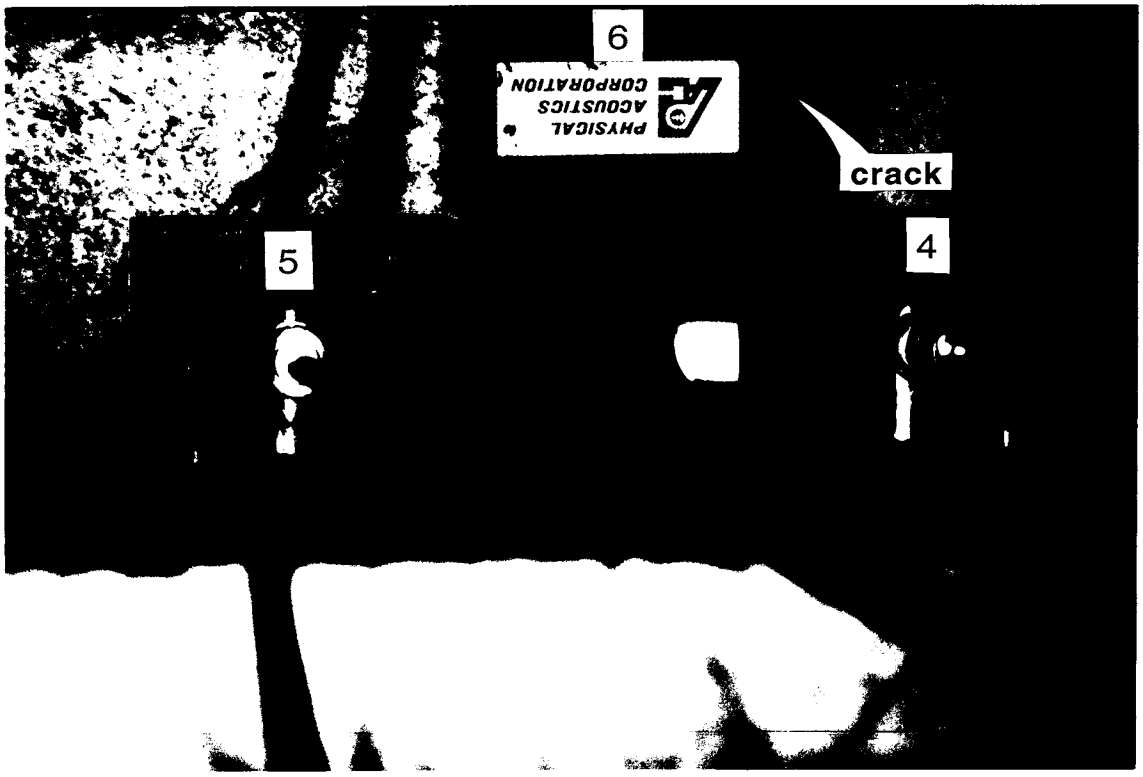

Figure 9. Close-up view of sensor placement at location 2 showing sensors 4, 5 and 6 positioned for triangular source location. Lower stop drill hole of crack is visible.

The sensor array at location 1 detected no events coming from the crack tip. The triangular array at location 2 detected no events at all. Figure 10 shows the detected events at location 2 when the pencil lead break tests were performed. The cluster of events at 3.5,.5 is a series of lead breaks done at the 6 o'clock position beside the lower hole, where a crack would be expected if it propagated past the drill hole.

The results showed that the crack at location 1 was not active during the monitoring period. Results also showed that the drill hole at location 2 successfully arrested crack growth. However, monitoring time was limited, the test was not done during rush hour, and the bridge was only loaded on one lane, so the results may not fully represent the general behavior of the cracks.

The main difficulty in this test was the limited space around the cracks available for sensor placement. The relatively large size of the R30I sensors and magnetic hold-downs limited the options for positioning the sensors. This affected source location accuracy and the ability to set up effective guard sensors. Instrumentation, particularly the sensors, needs to be adaptable to each individual application.

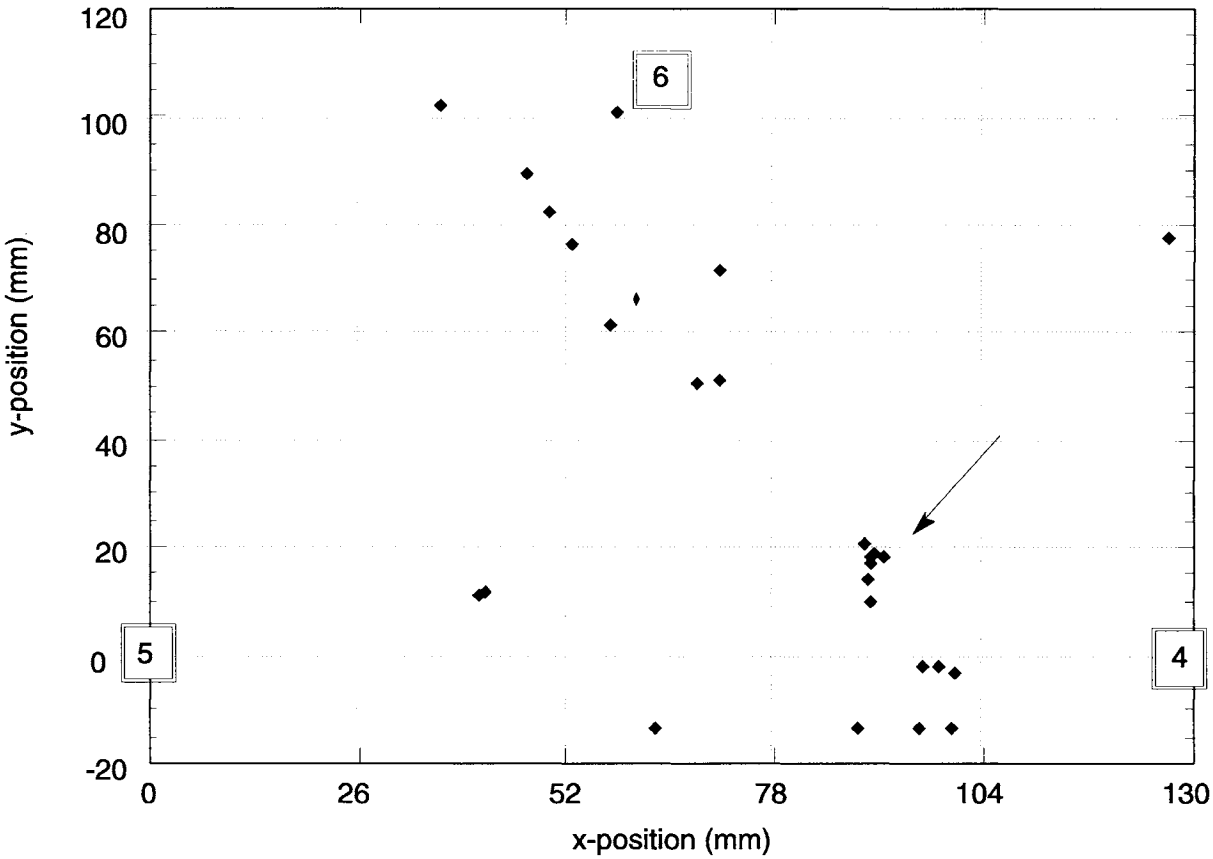

Figure 10. Triangular source location plot of pencil lead breaks at location 2. Arrow points to lead breaks done below the lower stop hole.

Case 3: Moormans River Bridge

The Rt. 671 bridge over the Moormans River in Albemarle County (Figure 11) was monitored on July 27, 1994. A load limit of 3 tons had been posted for the bridge, due in part to a crack on one of the 19 mm (3/4 ") square diagonal counters (Figure 12). This was the only defect monitored for AE.

The part monitored had a simple geometry and the crack was well separated from possible noise sources. Noise could propagate only from the ends of the bar. Two R30I sensors were attached 152 mm (6 in) apart on opposite sides of the crack. These sensors were set up to do linear source location. A WD sensor for recording waveforms was mounted close to the crack on the opposite side of the bar.

The AE equipment was set up away from the bridge. Being on a secondary road, the bridge was loaded very intermittently. The crack was monitored for about 1.5 hours during a steady rain.

Although AE was detected every time a vehicle passed, only three events were recorded by the source location program, none of which came from the location of the crack. The triggering threshold of the TRA had been set at absolute minimum, yet no signals detected were strong enough to trigger it. No waveforms were recorded. The results show that the crack is benign and has become inactive. The unbroken appearance of the rust covering the crack tends to support this conclusion.

Figure 11. Rte. 671 bridge over the Moormans River in Albemarle Co., VA.

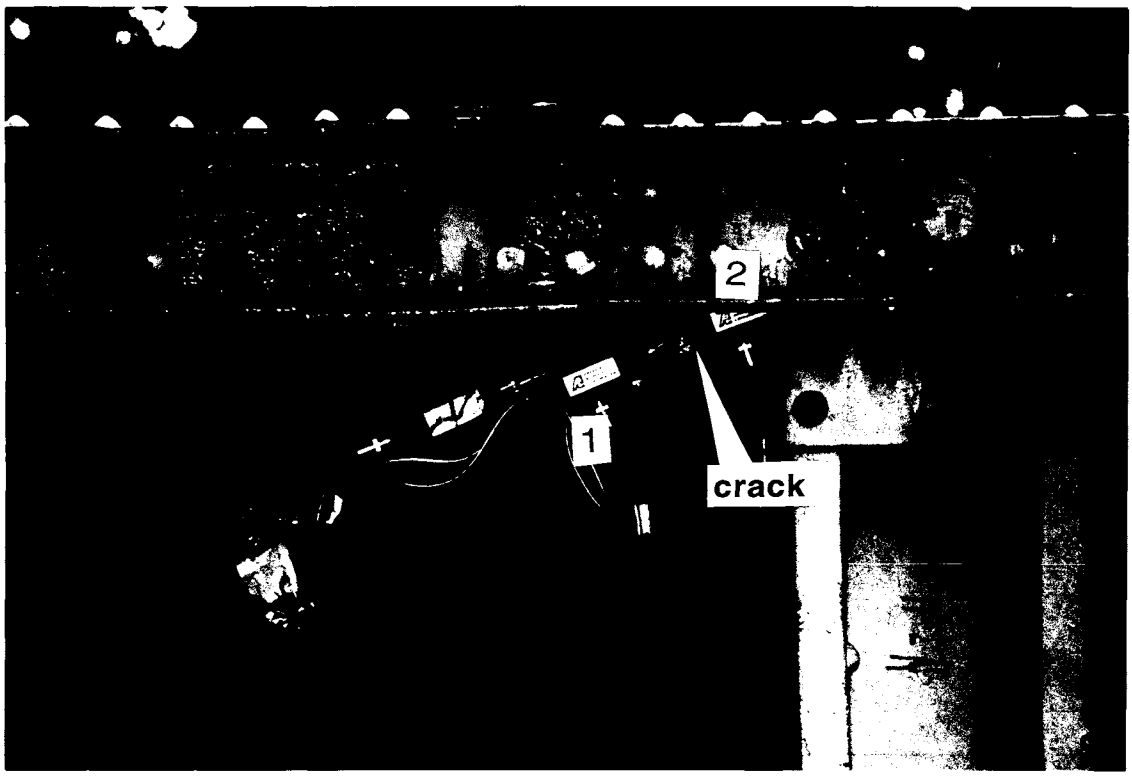

Figure 12. Sensor placement at the cracked diagonal counter.

Case 4: I-81 South Exit Bridge Over Rte. 29

The I-66 south exit bridge over Rte. 29 in Gainesville, VA was monitored on August 16,1994 (Figure 13). A truck passing under the bridge had accidentally hit the lower flange of the northernmost girder, causing the web and a stiffener to deform and the welds to crack. The girder was repaired by replacing the stiffener, heat-straightening the web back and rewelding the flange weld and damaged coverplate.

Repairs had just been completed before the AE test. Two R30I sensors, labeled 1 and 2, were attached to the coverplate for source location on the new weld (Figure 14). R30I sensor 3 was installed on the flange above the first array, as a guard sensor for sensors 1 and 2 and a linear source location sensor with sensor 4. Sensors 3 and 4 were set up to monitor the rewelded web to flange section. The remaining sensors, 5 and 6, were positioned as guard sensors (Figure 15) against noise coming from the floor beams. The WD sensor was mounted close to the coverplate weld to record waveforms.

The bridge riding surface was under repair at the time of the test. Only one lane was open to traffic, which had to be slowed down as the bridge was crossed. AE data was collected for 1 hour and 25 minutes.

Figures 16 and 17 show the results of source location for the two sensor arrays. Very few events were detected. The effects of guard sensors are also shown, although even without guard sensors the location findings detected no active cracks. No data was collected by the TRA, because even at minimum threshold settings, no AE detected by the WD sensor was strong enough to trigger the transient digitizer.

Although results from this particular AE monitoring test were negative for crack activity, this was not a reliable test of whether the repair of the damaged girder was successful. The bridge was not subjected to normal loading, and probably experienced less dynamic load during the test than in service.

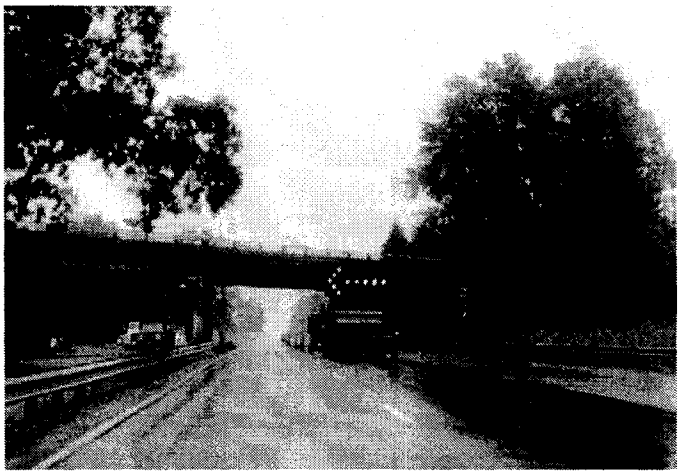

Figure 13. South exit bridge over Rte. 29 in Gainesville, VA

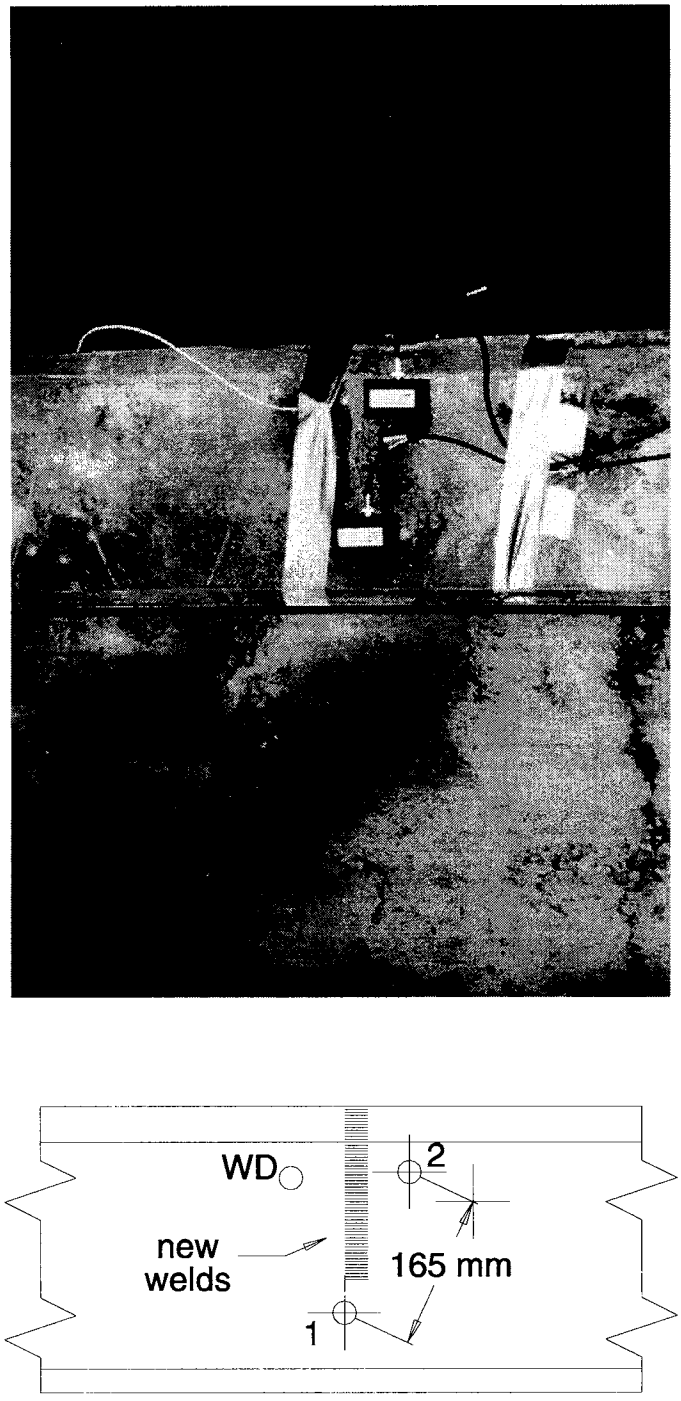

Figure 14. Sensor placement at coverplate showing sensors 1 and 2 positioned for linear source location to monitor new weld.

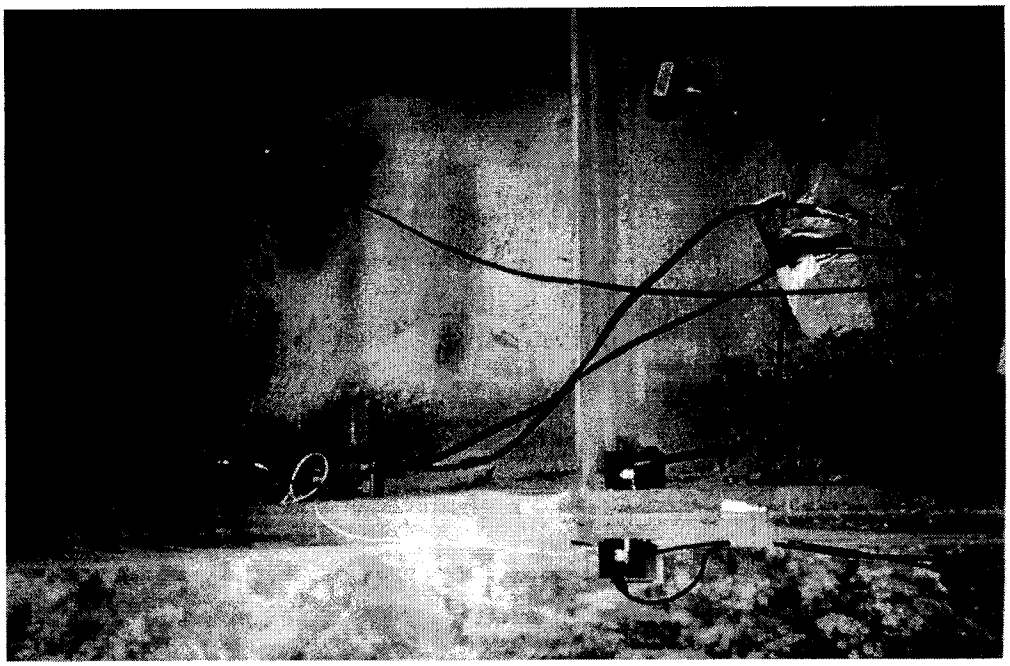

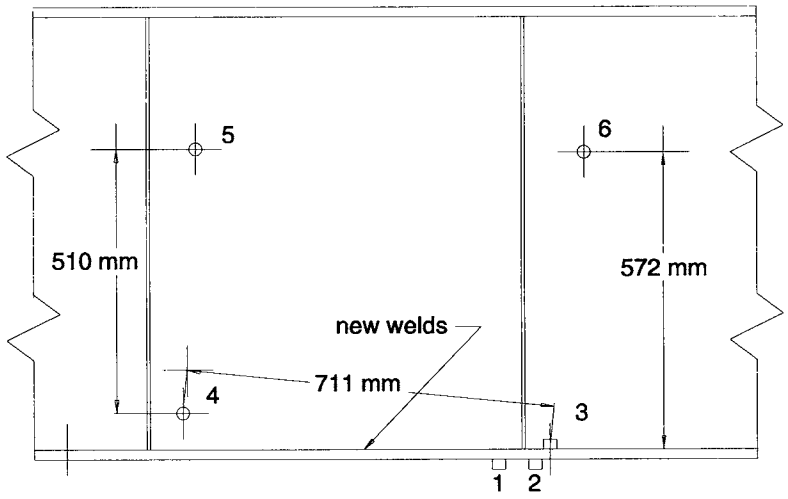

Figure 15. View of repaired girder showing location of sensors 3 and 4, positioned for source location to monitor lower flange-to-web weld, and guard sensors 5 and 6.

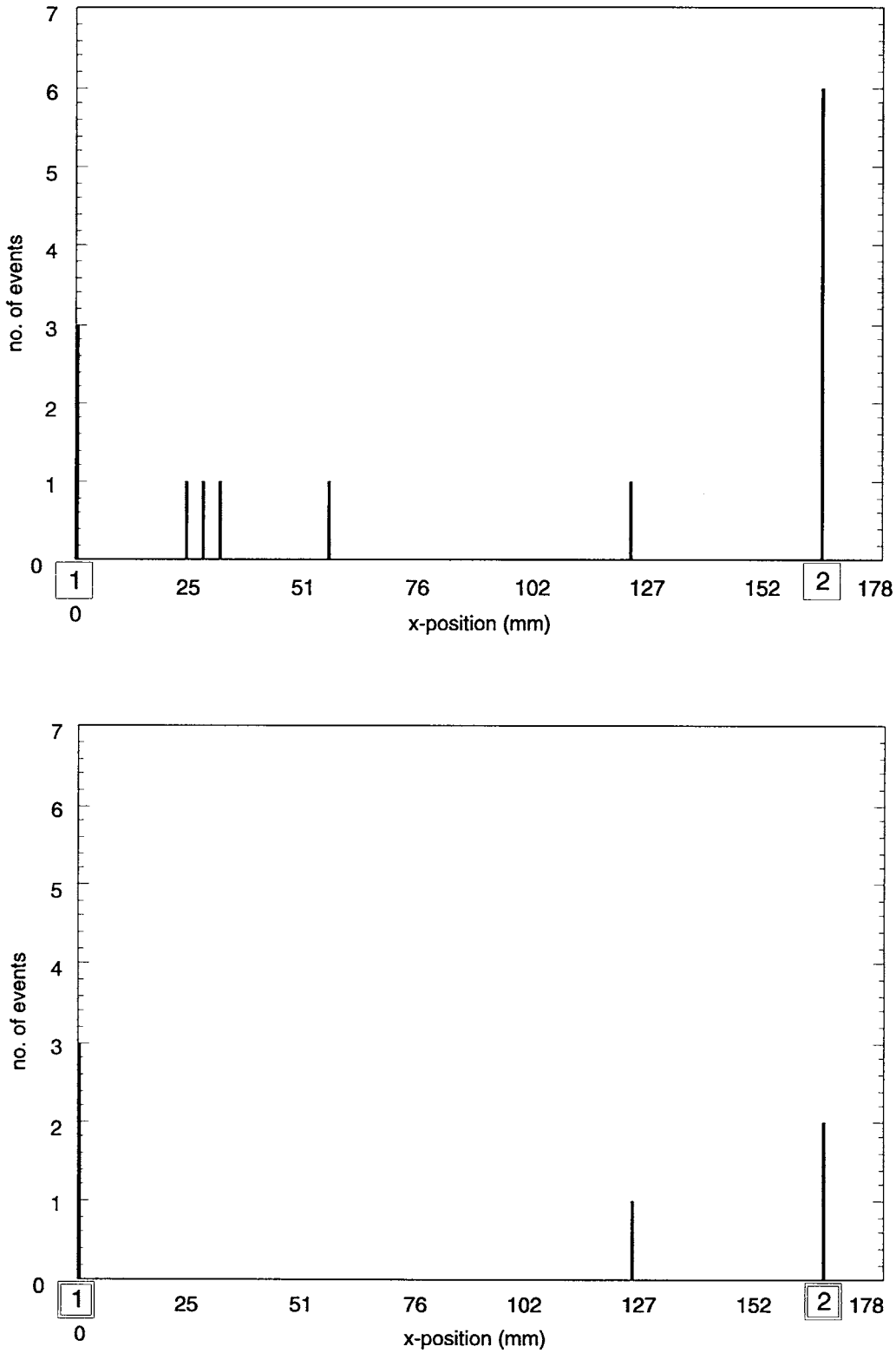

Figure 16. (Top) Source location results for the coverplate weld (without guard sensors) showing no evident crack activity, and (Bottom) the same location using guard sensors 3, 4, 5 and 6.

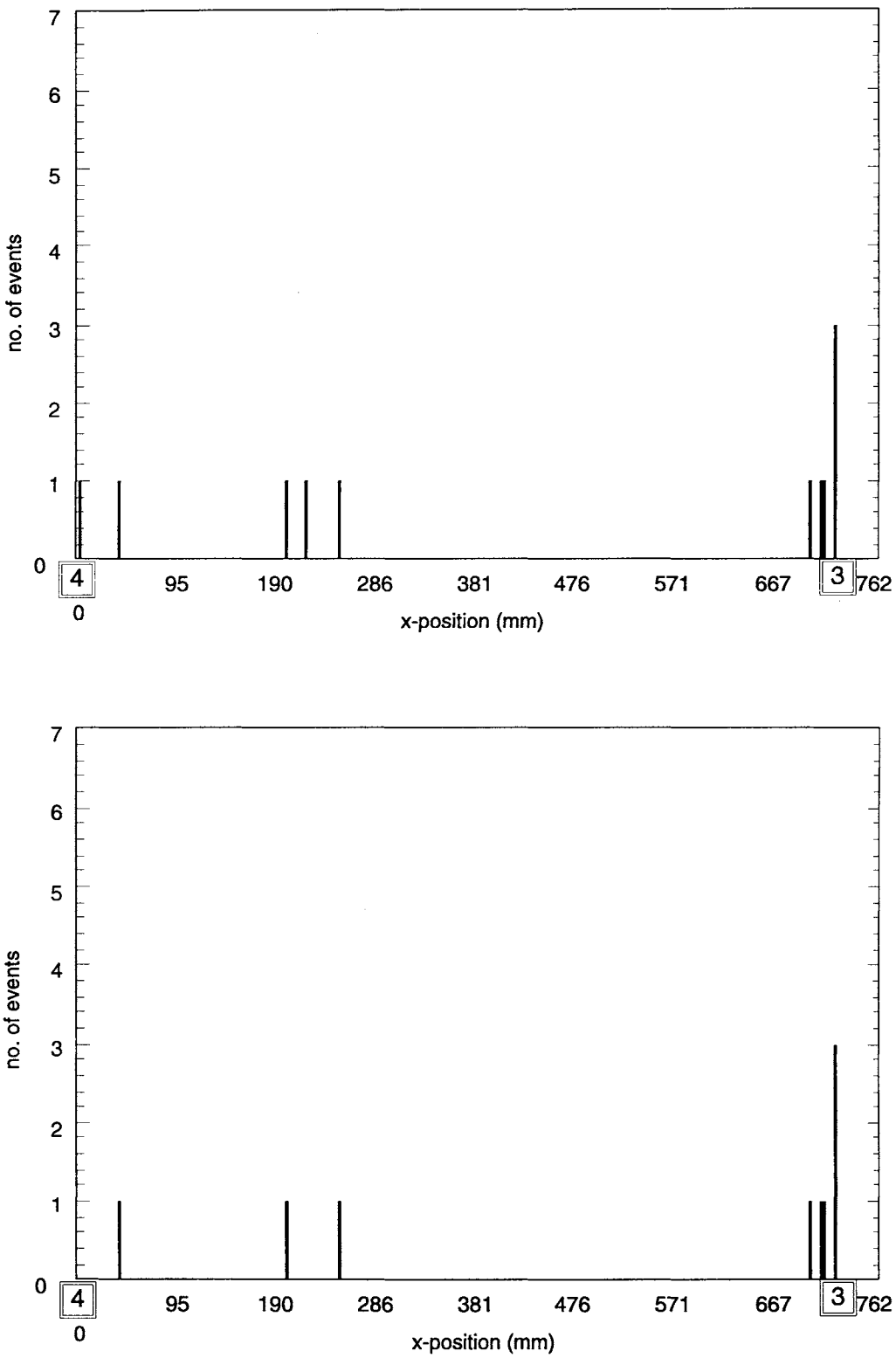

Figure 17. (Top) Source location results for the lower web-to-flange welds (without guard sensors) showing no evident crack activity, and (Bottom) the same location using guard sensors 1, 2, 5 and 6.

Case 5: Robinson River Bridge

The Rte. 29 northbound bridge over the Robinson River in Madison County, VA was monitored more extensively than any other bridge in this project. The bridge was tested on three occasions, June 24, Oct. 25, and Dec. 8 -9, 1994.

The bridge, built in 1934, has 4 steel girders extending over 5 spans with an overall length of 59 m (193 ft). The suspended span #2 (Figure 18) is supported by 8 pin-and-hanger connectors on the north end and by a pin joint on the opposite end. The 609 mm (24 ") high by 165 mm (6.5 ") wide hangers, with a 229 mm (9 ") x 64 mm (2.5 ") slot cut out from the middle, were fabricated from 16 mm (5/8 ") thick steel plate.

During a regularly scheduled inspection in October 1992, cracks were found on two of the hangers. The east exterior hanger had one 9.4 mm (0.37 inch) long crack. Three similarly located cracks were found on the west interior hanger. The longest was 36 mm (1-7/16 ") and the shorter upper crack was 6 mm (0.25 in) long (Figure 19). The third crack, which is not a through part crack, does not appear in the figure and was visible only at the surface of the internal slot. All the cracks initiated at this internal cavity at practically the same location. Bolted catch plates were installed on both hangers to prevent collapse in the event of sudden failure of the hangers.

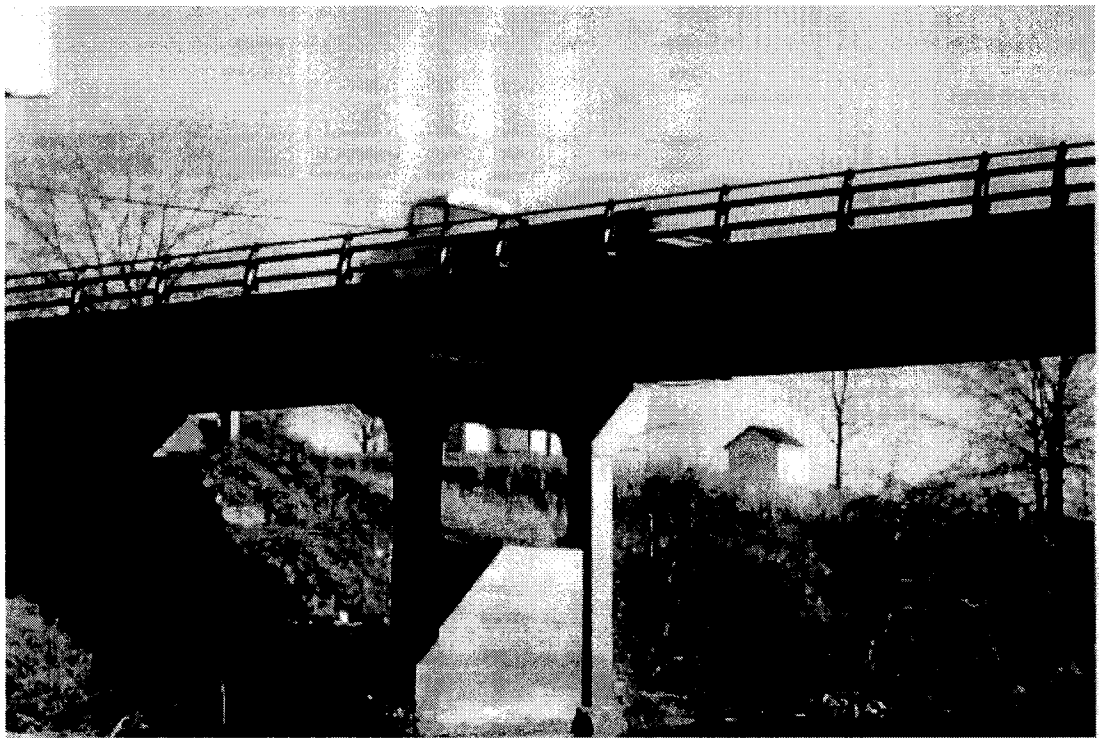

Figure 18. Rte. 29 north-bound bridge over the Robinson River in Madison County, VA.

June 24 Test

Both cracked hangers were monitored during the first AE test. An R30I sensor was attached as closely as possible to each crack. Sensor 2 was positioned close to the crack on the east hanger while sensors 1 and 3 were mounted on the ends of the pin (Figure 20). Sensors 4 and 5 monitored the two upper cracks and the lower crack on the west hanger (Figure 21). The WD wideband sensor 6 was installed on the top pin of the west hanger. Sensor placement was not originally intended to perform source location.

A Bridgemaster snooper truck was used to access the hangers when setting up the sensors. The truck was then taken off the bridge and both lanes cleared at the time of actual AE data collection. The bridge was loaded by normal noon-time traffic and data was recorded for a total period of 40 minutes.

In addition to AE recorded by the SA-LOC program, AE waveforms were also monitored and stored using the TRA-212 transient digitizer. One channel of the 2-channel system was assigned to the WD sensor while the other channel was used for the R30I sensors.

Although the test was not intended to include source location, analysis of the collected AE data made it apparent that spatial discrimination using source location was necessary to distinguish relevant AE signals from noise. Due to the irregularity of the sensor placement, the length of the effective wave propagation paths between the sensors could not be ascertained. This information was necessary for exact source location calculations. Still, using the differences in the time of arrival of an emission at two or more sensors as well as the sequence of arrival at the sensors, it was possible to get the approximate source location of the recorded AE events.

The results showed that a significant portion of all the detected AE events occurred close to sensor #4 at the upper crack, west hanger. Most signals were detected by only 1 or 2 sensors but the high amplitude events regularly hit three sensors (4, 5 and 7). The TRA data also showed that the highest amplitude signals originated there. Waveforms were collected from the WD sensor and sensors 1, 4, 5 and 6. The TRA was set at the lowest threshold possible, to maximize sensitivity. At this level, only the WD sensor and R30I sensor 4 detected signals that were recorded by the TRA. Apparently AE activity during the period of AE monitoring was greatest near the upper crack, although it could not be ascertained then if the AE signals were coming from the crack itself or from the nearby pin. These results were the basis for the decision to concentrate the monitoring effort on the upper crack of the west hanger in the next test.

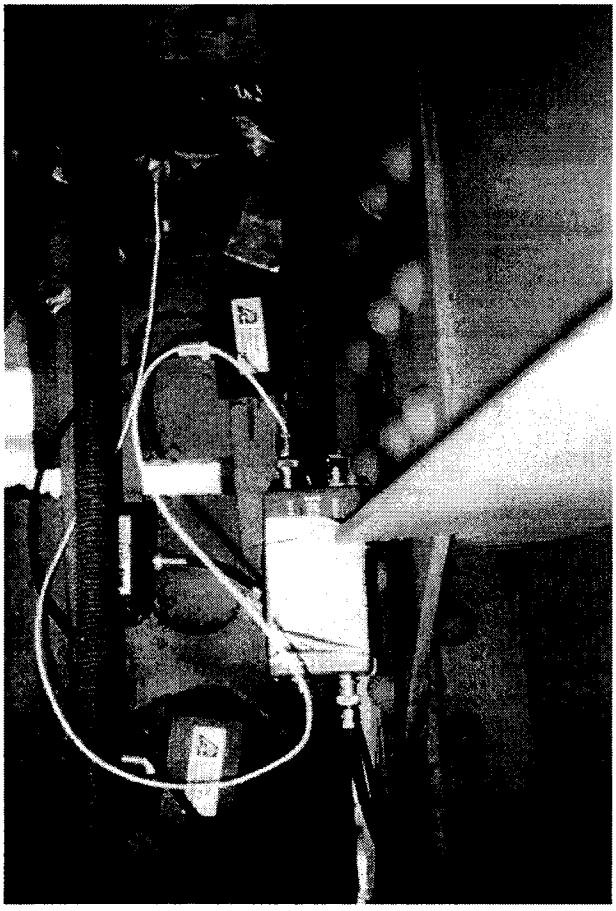

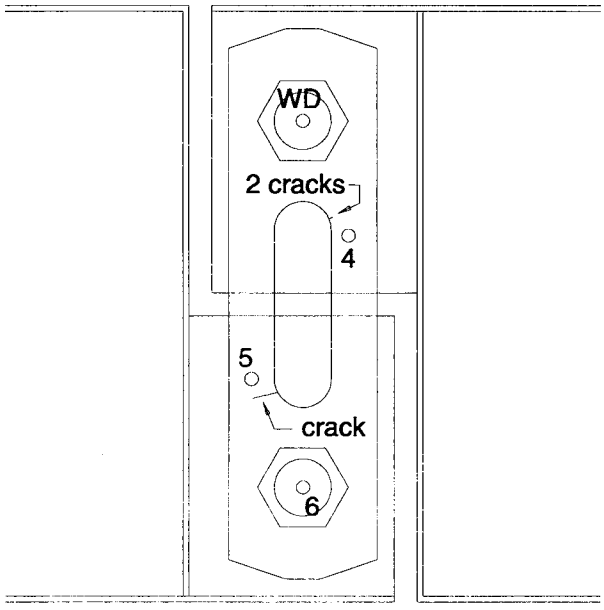

Figure 21. Sensor placement at west inner hanger for the June 24 test.

October 25 and December 8 & 9 Tests

AE Monitoring Set-up

Only the cracked west inner hanger was monitored on the second AE test of the Robinson River bridge. R30I sensors 3 and 4 were attached 178 mm (7 ") apart on both sides of the upper crack (crack #1) (Figure 22). The WD sensor used for recording waveforms was mounted between the R30I sensors close to the crack using cyanoacrylate adhesive. The other three R30I sensors were used as guard sensors to detect noise coming from outside the crack zone. Guard sensor 1 was positioned to eliminate rubbing noise from the top pin while sensor 6 was used to eliminate noise from the lower pin and AE from the lower crack (crack 2). Sensor 5 was mounted on the girder connector plate to filter out noise from the girder itself.

Unlike the first AE test, where AE parameters and AE waveforms were recorded at separate times, this test ran the SA-LOC with the TRA program in the background, so both systems recorded the same AE events. To increase the sensitivity of the TRA waveform recorder, an additional preamplifier was connected between the signal cable from the sensor and the TRA input. The pre-amps were set at 40 dB gain. One TRA channel was used for the WD sensor while sensor 3 was connected to the other TRA channel. A digitization rate of 5 MHz was chosen and the threshold levels were set to trigger the TRA system only when a vehicle passed over the bridge. Waveform size was set at 8K points which, at a pre-trigger delay of 10%, allowed the recording of 1.47 msec segments. For the SA-LOC, the threshold level had to be set at 30 dB to avoid low intensity background noise.

The AE monitoring setup in this test was further improved by using a strain gage. The strain gage was attached on the left side of the link (Figure 22). Its conditional output was connected to the Spartan and recorded as parametric input #1. Thus, in addition to spatial discrimination, the setup included strain discrimination as an additional tool for distinguishing between fretting noise, crack face rubbing and crack extension AE.

Dirt and corrosion products had accumulated and hardened between the hanger and the girder web extension beneath the crack. Since these products can produce noise AE not isolatable from crack AE by spatial discrimination, the space between the link and the girder was carefully cleaned. To further decrease the possibility of fretting noise coming from the vicinity of the crack, the area was sprayed with WD-40 lubricant.

As in the first AE test on this bridge, the Bridgemaster was used to set up the sensors and strain gage. Both lanes were again cleared and the bridge was loaded by normal bridge traffic during AE data acquisition. Total monitoring time was 1 hour and 35 minutes.

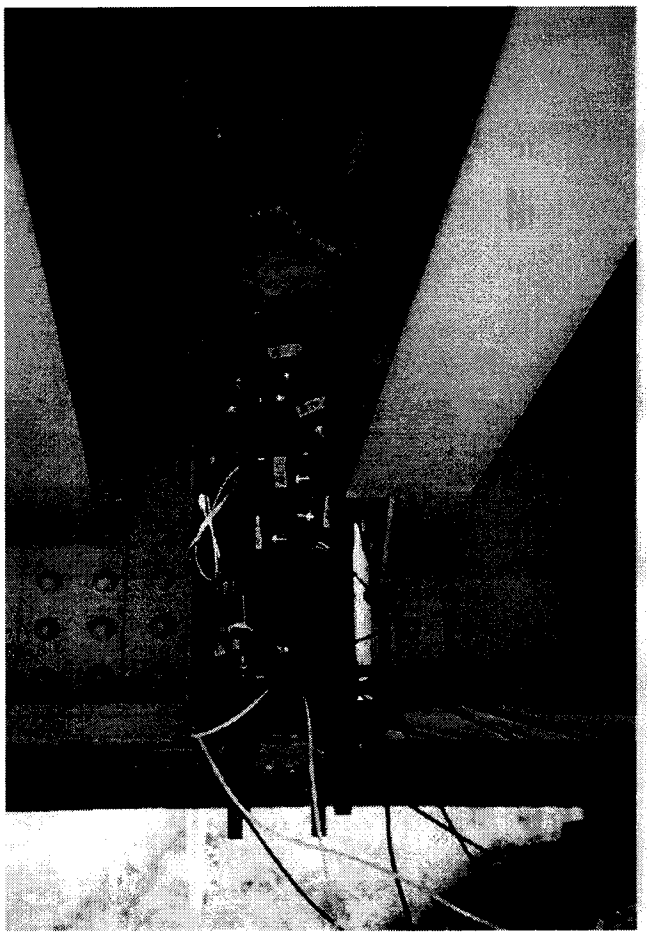

Figure 22. Sensor placement at the west inner hanger used to monitor crack #1 during the Oct. 25 test. Strain gage location is also shown.

The third AE test on the Robinson River Bridge gathered more AE and waveform data from crack #1, and also monitored the longer crack #2. Accordingly, the sensors were set up in two ways and monitoring time was divided between the two set-ups. In the first test, which was done on December 8 and part of December 9, the sensor placement was similar to the Oct. 25 test except that another R30I sensor, sensor 2, was attached close to the lower pin so source location could be performed on crack #2. This sensor also doubled as a guard sensor for the source location sensor array at location 1. Sensor placement is shown in Figure 23. Sensor 5 had to be disabled since the maximum number of operating channels had been reached. Results of the Oct. 25 test showed that guard sensor 5 was not necessary. Accidently, the distance between sensors 3 and 4 was increased to 184 mm (7.25 ").

In the second sensor arrangement scheme (Figure 24), the WD sensor was moved close to crack #2 so AE signal characteristics and waveforms from this crack could be recorded. Guard sensor 1 was attached to the end of the lower pin while guard sensor 3 was used to eliminate noise coming from the upper pin. Sensors 2 and 6 remained in the same position for linear source location on crack #2. The TRA channels were connected to the WD sensor and R30I sensor 6.

The strain gage was kept at the same location as on the Oct. 25 test. The threshold setting on the SA-LOC was decreased from 30 dB to 25 dB, because the first test showed that some crack-related signals had peak amplitudes less than 30 dB. TRA threshold levels were likewise adjusted so weak, long-duration noise signals would not be detected. The digitization rate was kept at 5 MHz while waveform record lengths were decreased to 1.17 msec for the WD sensor and 0.778 msec for the R30I sensor on the basis of results from the previous test.

At the time of this test, a wooden platform was installed under the bridge to provide the AE team unassisted access to the west inner link. At all times during sensor setup and testing and actual monitoring, both lanes of the bridge were open to loading from passing traffic.

The hanger was monitored for a total of 44 minutes on the first day using the first sensor arrangement and again for a total period of 1 hour and 35 minutes on the next day. Sensors were then rearranged to the second set-up scheme and data was collected for 22 minutes. Monitoring times were not continuous; on occasion, data was only collected when large vehicles such as tractor-trailer trucks passed over the bridge.

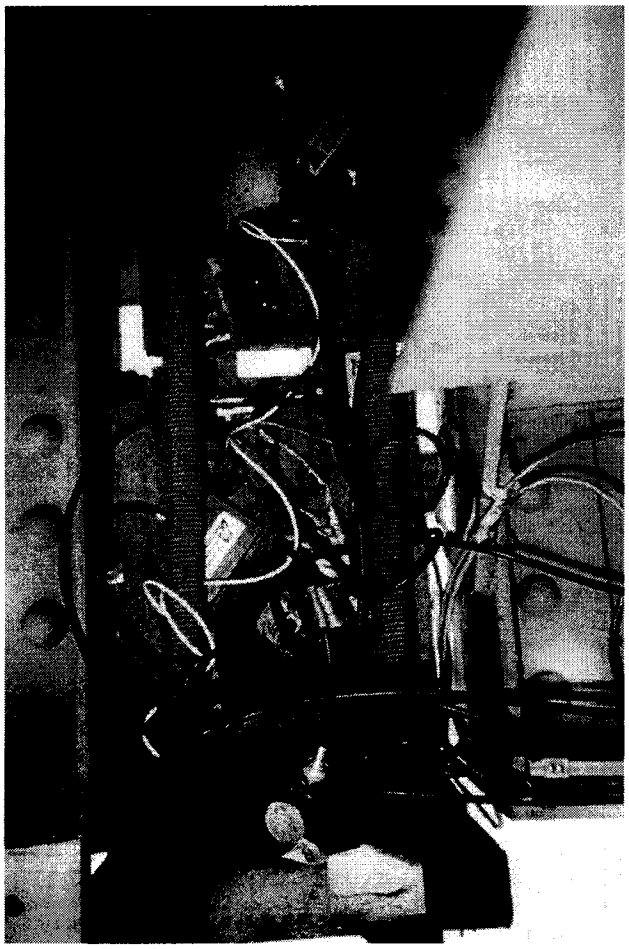

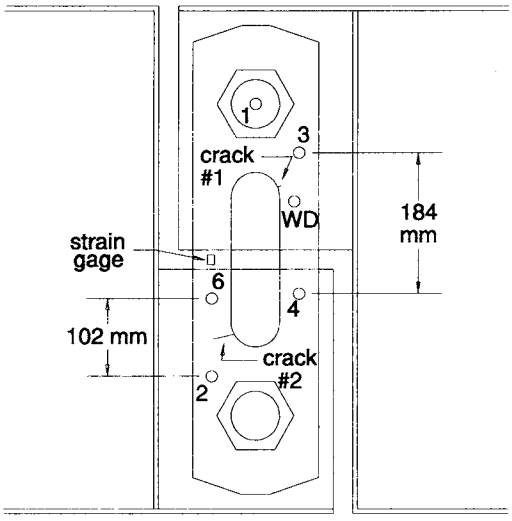

Figure 23. Sensor placement used to monitor crack #1 during the Dec. 8 and 9 tests, showing sensors 3 and 4 positioned for linear source location, and guard sensors 1, 2 and 6. Sensors 2 and 6 double as source locators for crack #2. Also shown is the wideband sensor close to crack #1 and the strain gage location.

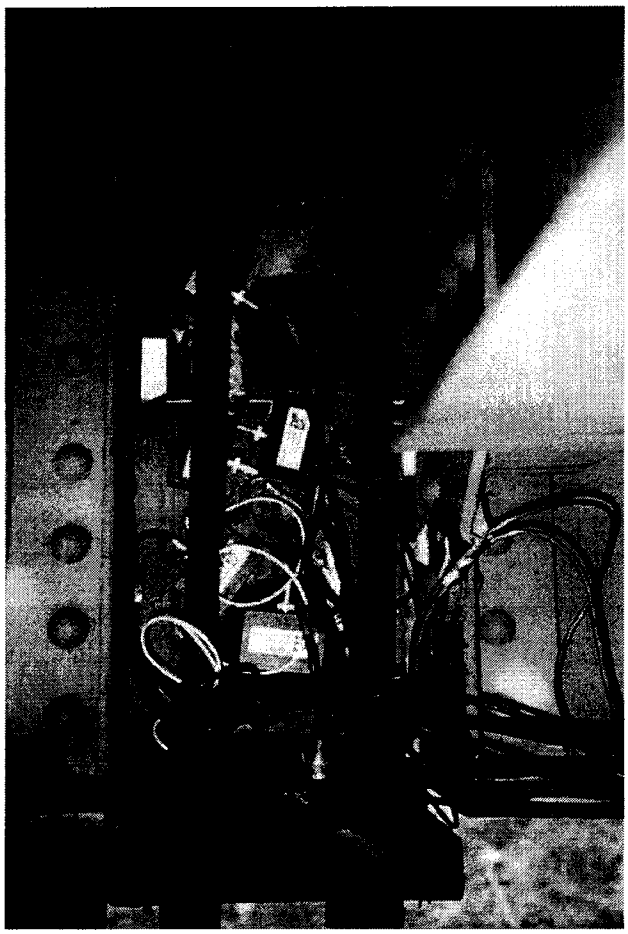

Figure 24. Sensor placement used to monitor crack #2 during the Dec. 9 test showing sensors 6 and 2 positioned for linear source location, and guard sensors 1 and 3. Also shown is the wideband sensor close to crack #2 and the strain gage location.

Spatial Discrimination

The June 24 test indicated a strong AE source close to crack #1, although failure to arrange the sensors for source location made it impossible to determine whether the signals were crack-related or were fretting noise from the pin. The results of linear source location on this crack for the October 25 test are shown in Figure 25 (Top). These were combined from multiple testing periods totaling 1 hr and 35 minutes. Only 83 events were detected, but even with this dearth of activity a clustering of events can be recognized between x = 40.6 and 45.7 mm (1.6 and 1.8 in), where the crack was located. This is clearer in Figure 25 (Bottom), where signals that hit the guard sensors first are eliminated from the plot.

Although sensors 3 and 4 were intended for source location, the WD sensor could also serve this purpose in conjunction with one or both of the R30I sensors. This was handy when a crack-related event detected by the WD sensor was detected by either sensor 3 or 4 but not by both. Analysis of time-of-arrival data showed this to be the case. Seven more crack-related events were identified using the WD sensor as a locator.

The threshold setting on the December 8 and 9 test was 5 dB lower than the setting used on Oct. 25, which partly explains why more events were detected during the 44 minutes that crack #1 was monitored than during the longer test period on Oct. 25. Figure 26 shows the location of these detected events. The effectiveness of the guard sensors is more evident here, as shown by the removal of most of the signals that appeared close to sensor 4. Most of the signals eliminated by the guard sensors came from a source closest to sensor 6, which had the greatest number of signals detected of all the sensors.

Source location results from the same sensor 3 and 4 array in the Dec. 9 test (Figure 27a) came as a surprise. The expected cluster of events at the crack #1 location was absent. Instead, events were concentrated around x = 6 mm (0.4 in). These signals are believed to have been generated by the other crack close to and right above crack #1, referred to as crack #3. A plot of events that passed the guard sensors is shown in Figure 27b, where crack-related AE from crack #3 becomes even more apparent. As in Figure 26, most of the events excluded by the guard sensors came from a source closest to sensor 6. Both plots demonstrate the need for guard sensors in monitoring crack #1. Of the 997 total events detected by the sensor 3 and 4 array, 566 events or 56.8% of the total were eliminated by the guard sensors.

Figure 28 shows a sample of events located by sensors 2 and 6, the array configured for linear source location on crack #2. The plot displays 247 events, all of which were detected when a single tractor-trailer truck passed over the bridge. Crack #2 was obviously much more active than the other 2 cracks. In one 30-minute continuous monitoring period, 4670 events were detected at location 2, and only 57 from location 1. The data for Figure 28 were collected using the second sensor arrangement, where guard sensors 1 and 4 were positioned to reject outside noise, notably fretting noise from the pins. However, for the particular test referred to in the location plots, only 10 events were rejected by the guard sensors. Guard sensors had less impact and were less important in monitoring crack #2.

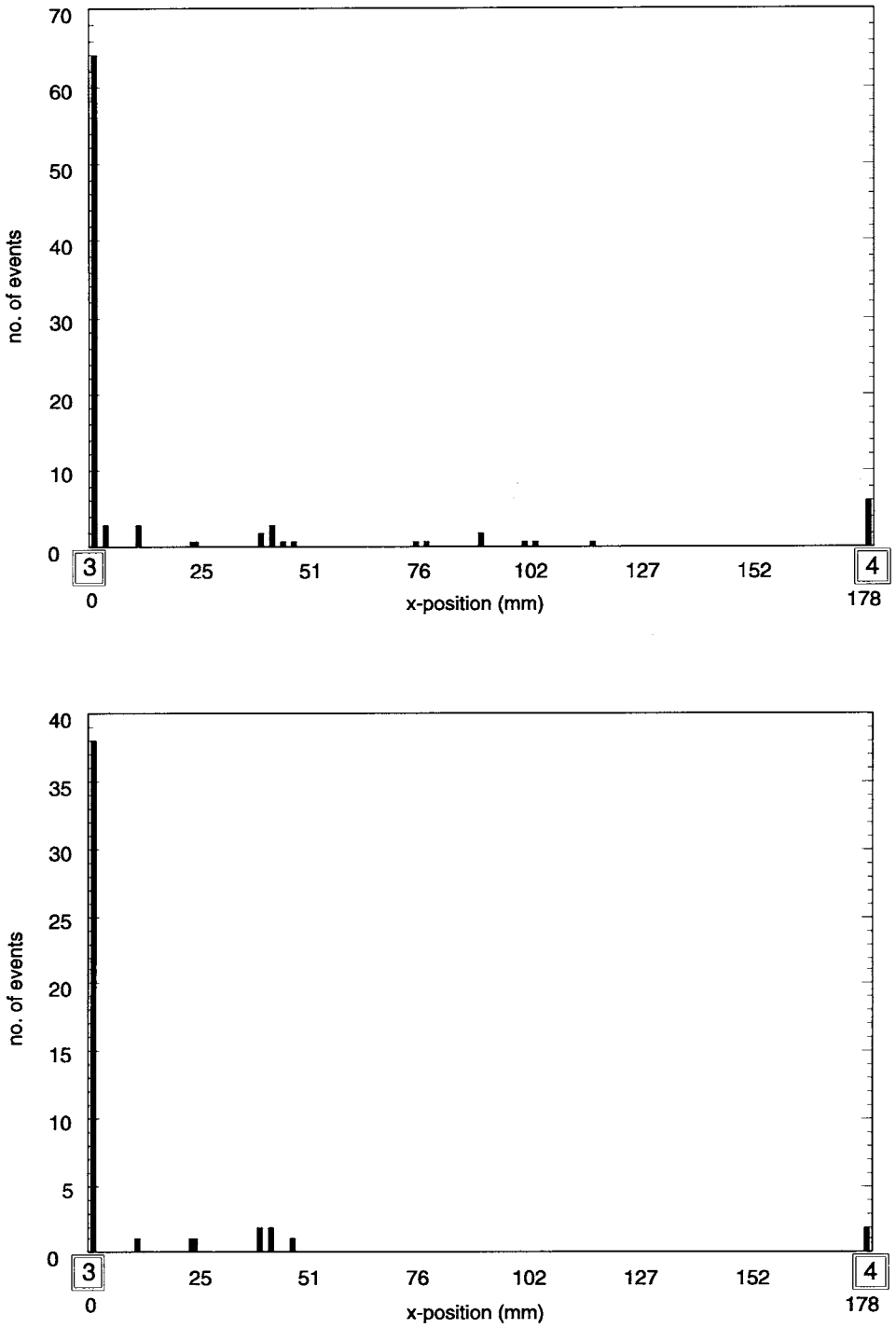

Figure 25. (Top) Source location results for the Oct. 25 test (without guard sensors) showing events at crack location between 45 and 50 mm. (Bottom) The same location using guard sensors 1, 5 and 6.

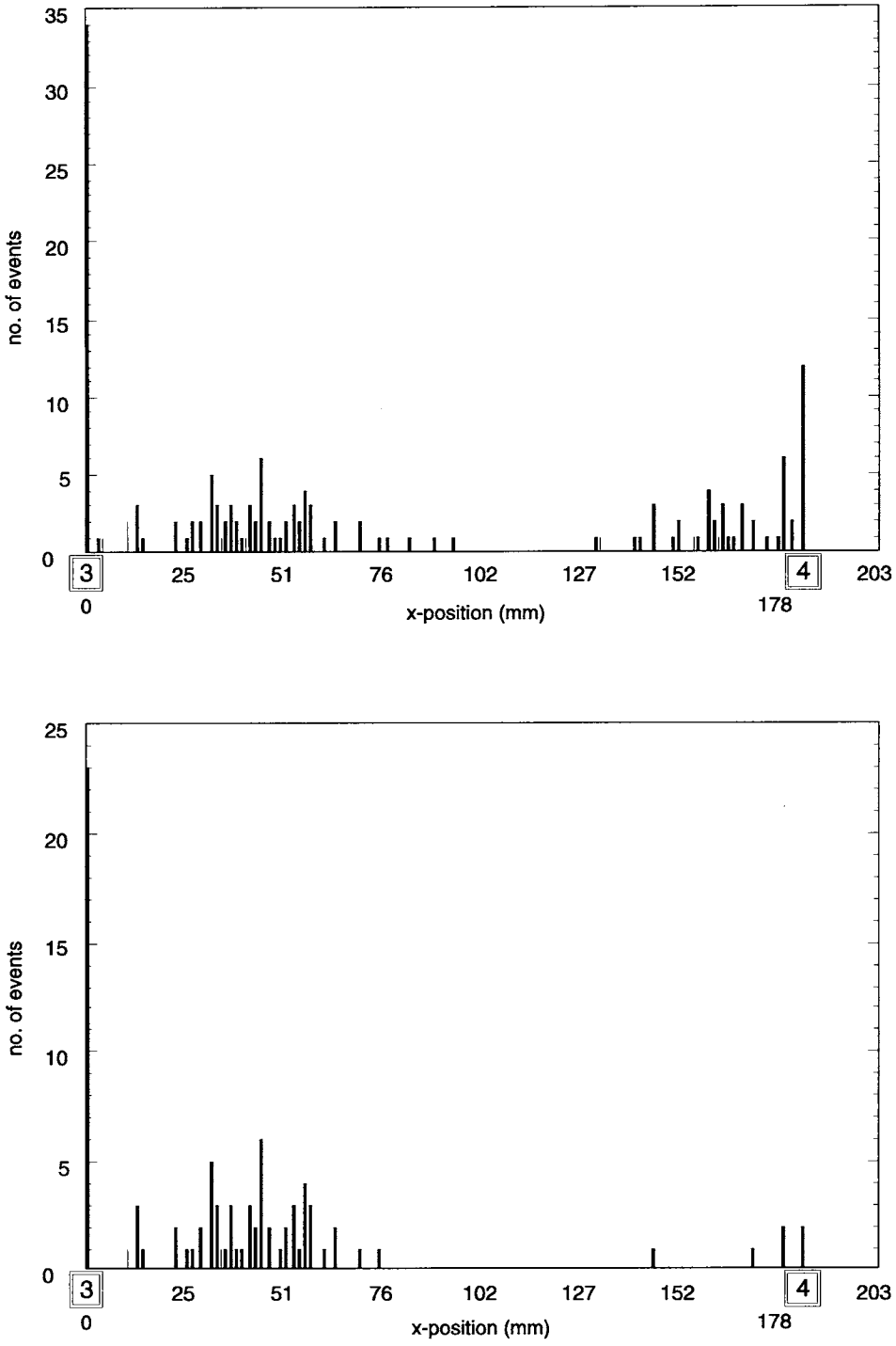

Figure 26. Location of detected events for crack #1 in Dec. 8 and 9 test.

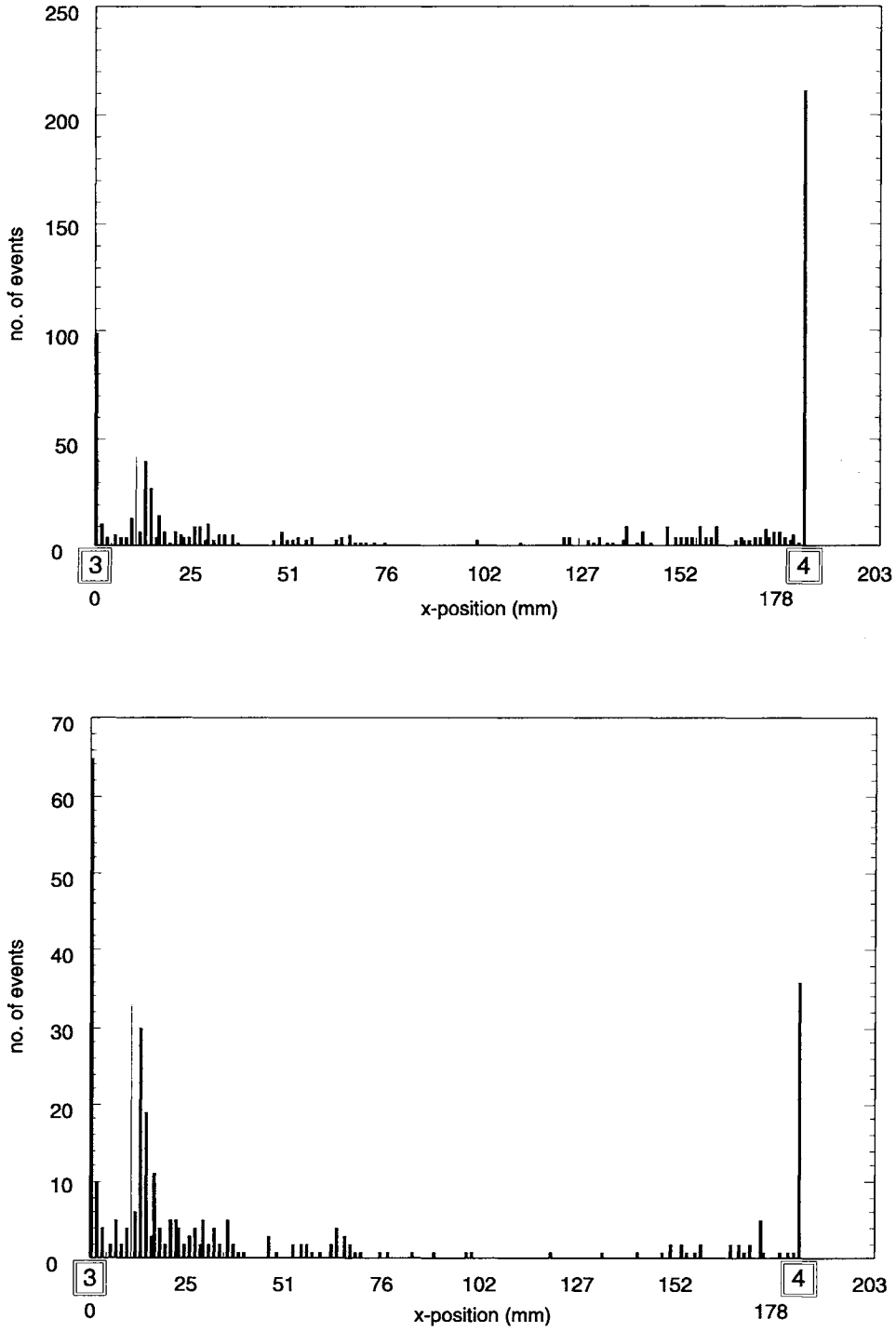

Figure 27. (Top) Source location results from Dec. 9 monitoring of crack #1 (without guard sensors) showing cluster of events at crack #3 location. (Bottom) The same location using guard sensors 1, 2 and 6.

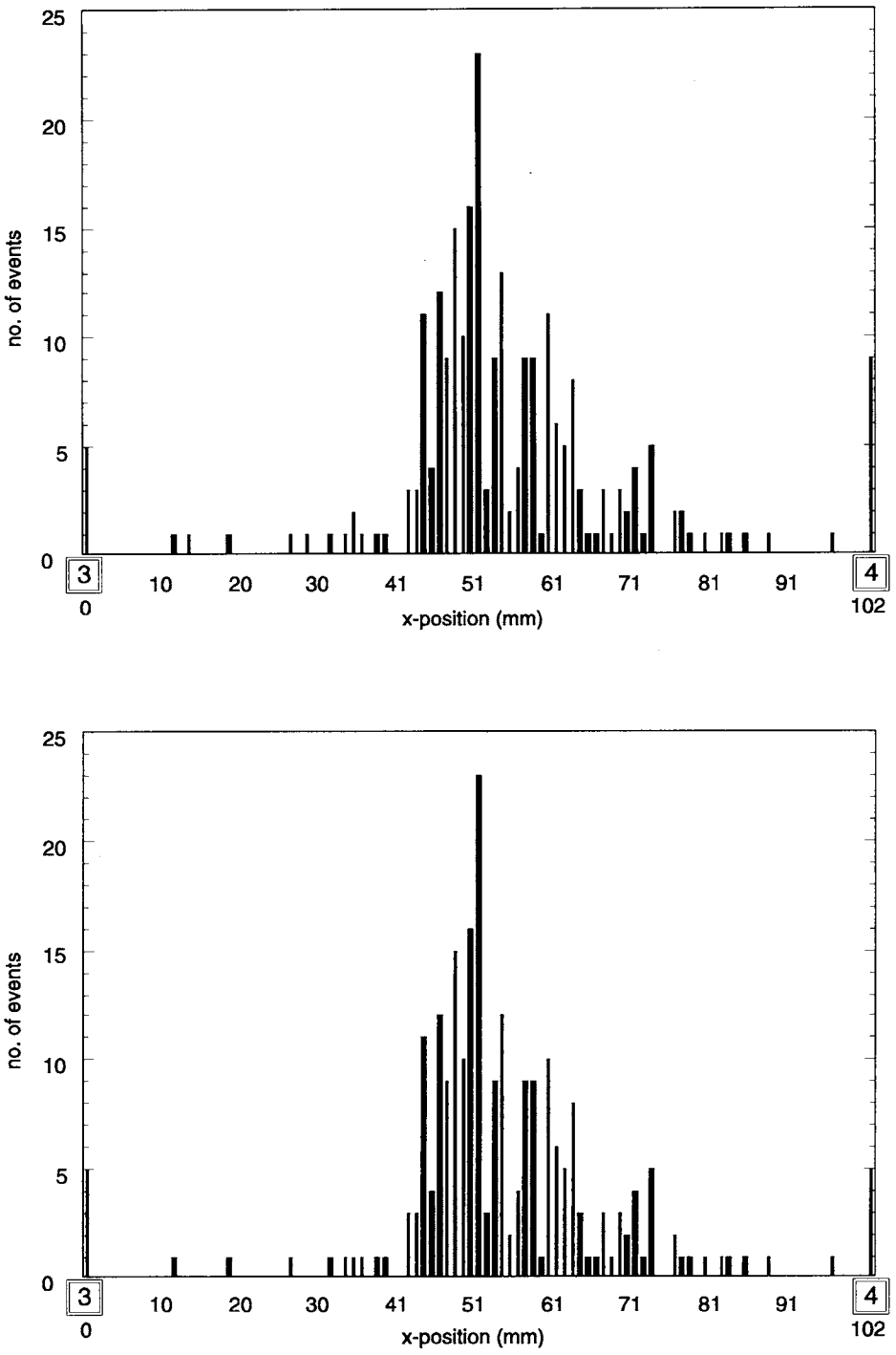

Figure 28. Events located by sensors 2 and 6, configured for linear source location on crack #2.

The events in Figure 28 are more spread out than expected. The accuracy of the source location function of the data acquisition system was undoubtedly a factor in this spread. However, another explanation is that many of the located events were due to crack face rubbing which may have occurred anywhere along the 36 mm (1-7/16 ") long crack faces. A longer crack surface, with more rubbing surfaces, can also partly explain the larger number of detected events compared to the shorter cracks #1 and #3.

Waveform and Frequency Analysis

A prime advantage gained from operating both SA-LOC and TRA simultaneously is the ability to record an entire waveform while determining the location of the AE event. That is, both spatial and frequency discrimination techniques become available for distinguishing defect-related AE from noise. Storing strain gage data with the data acquisition system adds a load discrimination capability. The Oct. 25 test benefitted from both these advantages.

Waveforms of 11 crack-related events from crack #1 were stored from the Oct. 25 test. Figure 29 shows a representative waveform as detected by the wideband transducer, together with its normalized frequency spectrum. Figure 30 shows a typical noise waveform and its frequency spectrum as detected by the WD sensor. All of the crack-related AE signals had nearly the same waveform envelope shapes. However, the most notable feature distinguishing crack-related AE from noise is the peak frequency. All the crack signals had peak frequencies of 275 KHz, while all other waveforms, assumed to be noise, peaked no higher than 200 KHz, mostly less than 100 KHz. This, it should be noted, applies only to signals recorded from the WD wideband sensor. Figures 31 and 32 show the same crack and noise emissions as detected by R30I sensor 3. Both waveforms have frequency contents that peak at about 325 KHz, which is close to the transducer resonant frequency. This clearly illustrates how the R30I resonant sensor modifies the AE signals it detects with its own characteristics, thereby masking the inherent differences between crack-related AE and noise.

In the Dec. 8 and 9 tests, waveforms from both cracks #1 and #2 were recorded. Crack #1 waveforms had more variability than previously observed but are generally similar to those recorded on Oct. 25, including the characteristic peak frequency. One difficulty normally encountered in AE testing is the reproducibility of results. One factor, among others, is the care taken in properly installing the sensors, and the results indicate that this was adequately addressed.

More waveforms were recorded from crack #2 than from crack #1. Figures 33 to 36 show representative crack-related and noise waveforms with their corresponding normalized frequency spectra. These waveforms, unlike those recorded from crack #1, cannot be as easily classified into two main categories. The crack-related signals, besides having a strong component in the 200 to 300 KHz range, also have significant low frequency components (Figure 33). The waveform shows that the signal starts out at high frequency with the low frequency components becoming more evident as the signal decays. This is also displayed by the noise waveform of Figure 34 although the high frequency oscillations die out sooner. Both waveforms are longer than the crack-related waveform from crack #1.

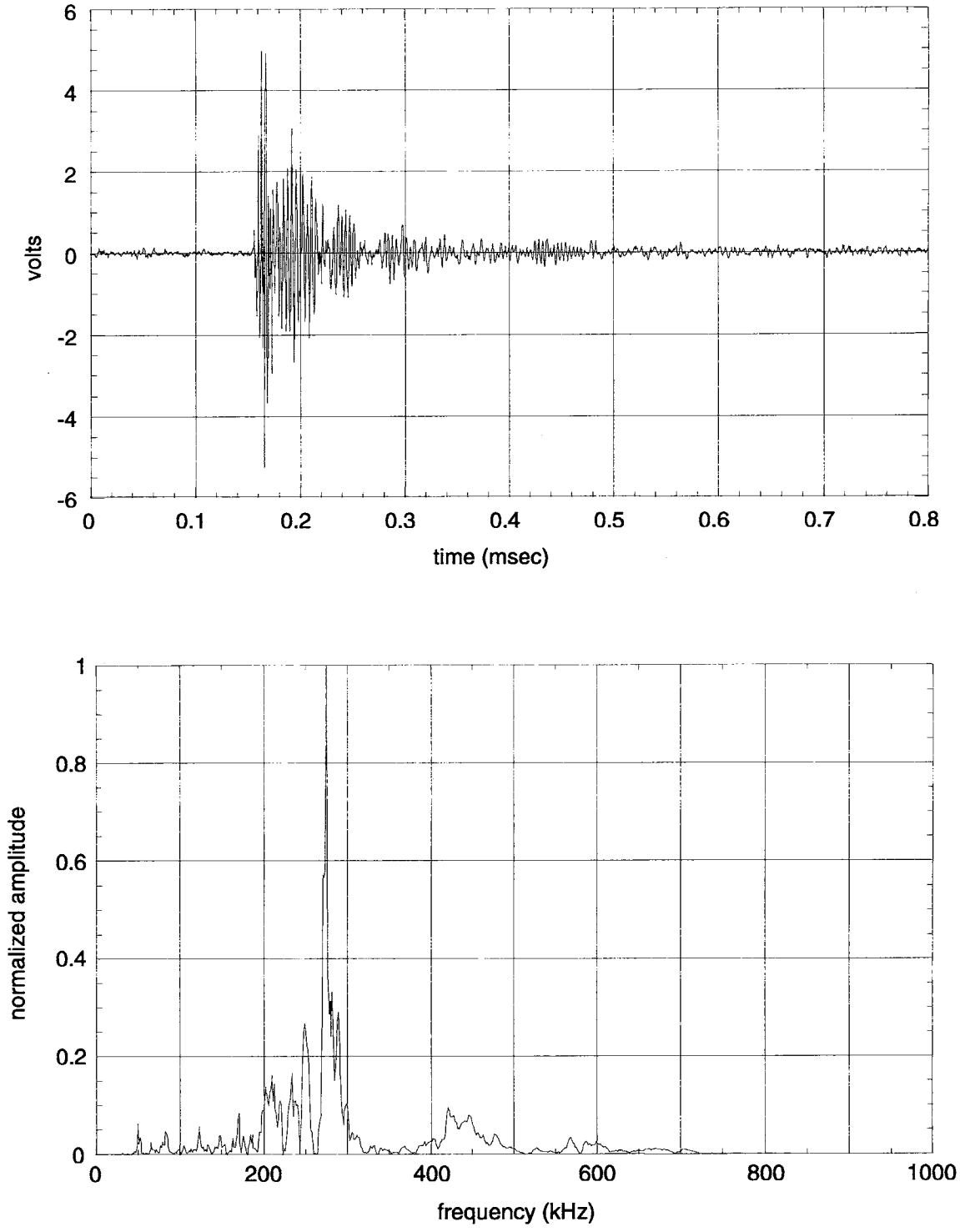

Figure 29. Wideband (WD) sensor waveform and normalized FFT of crack-related AE from crack #1.

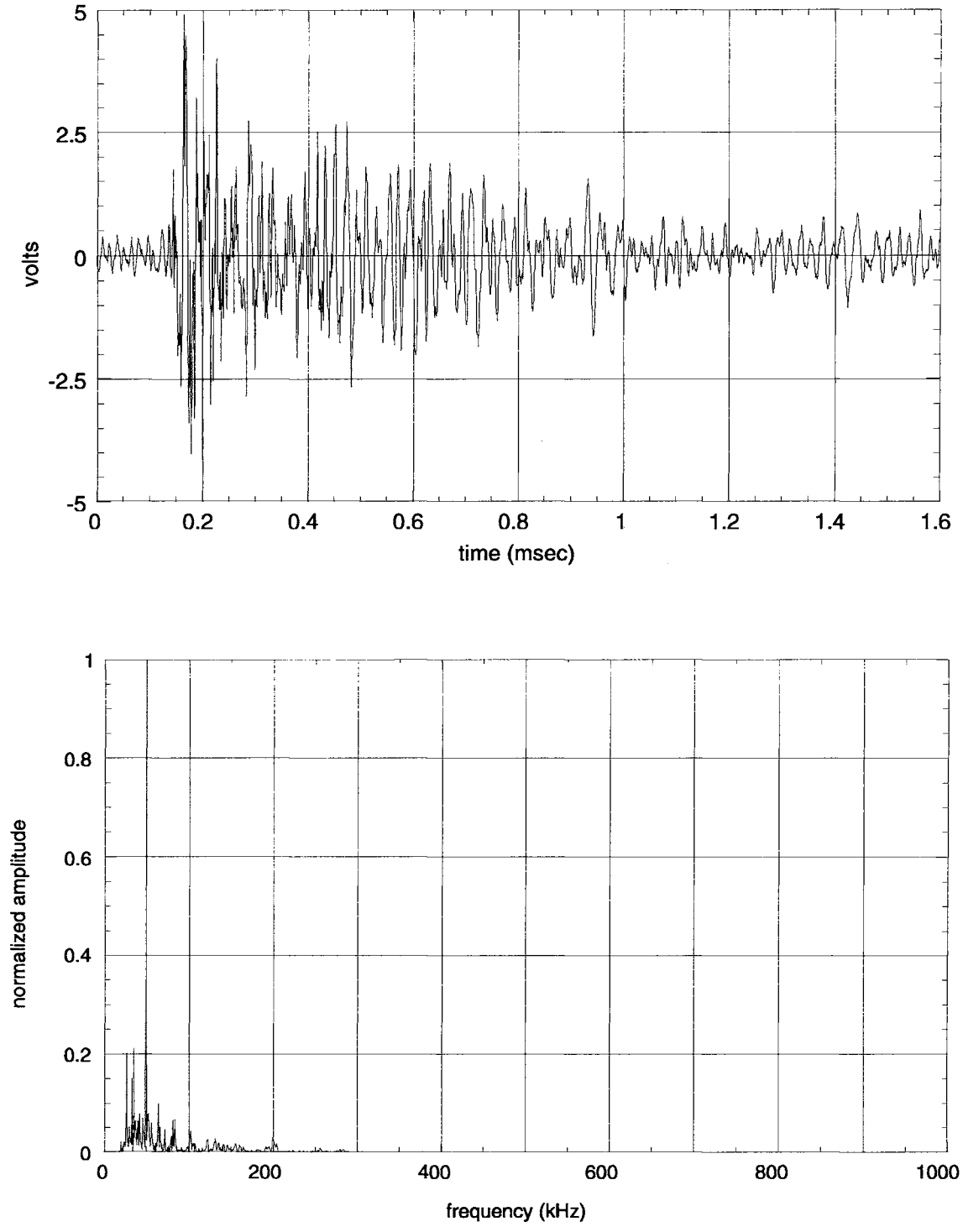

Figure 30. Typical noise waveform and its frequency spectrum as detected by the WD sensor.

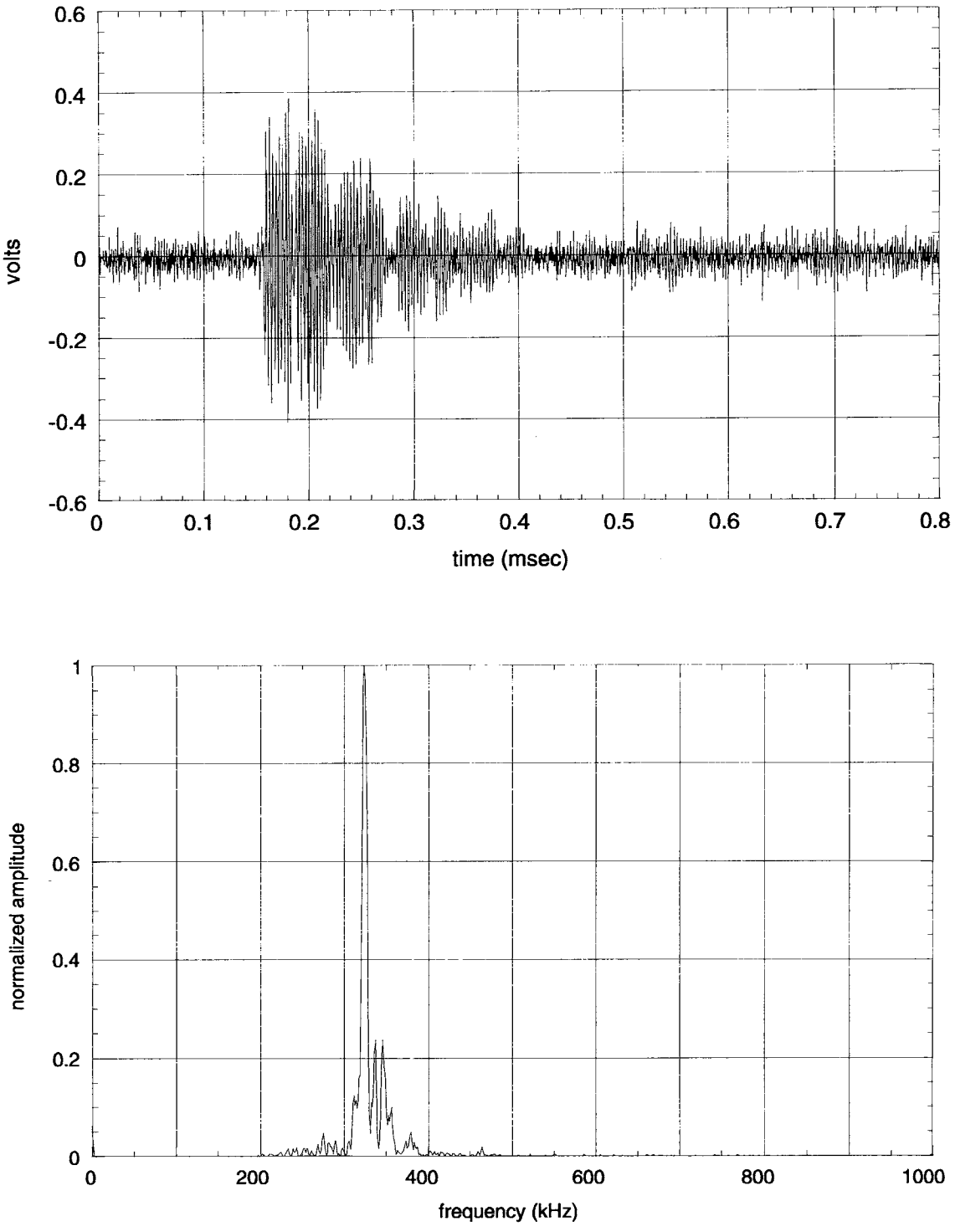

Figure 31. Resonant (R30I) sensor waveform and normalized FFT of crack-related AE from crack #1.

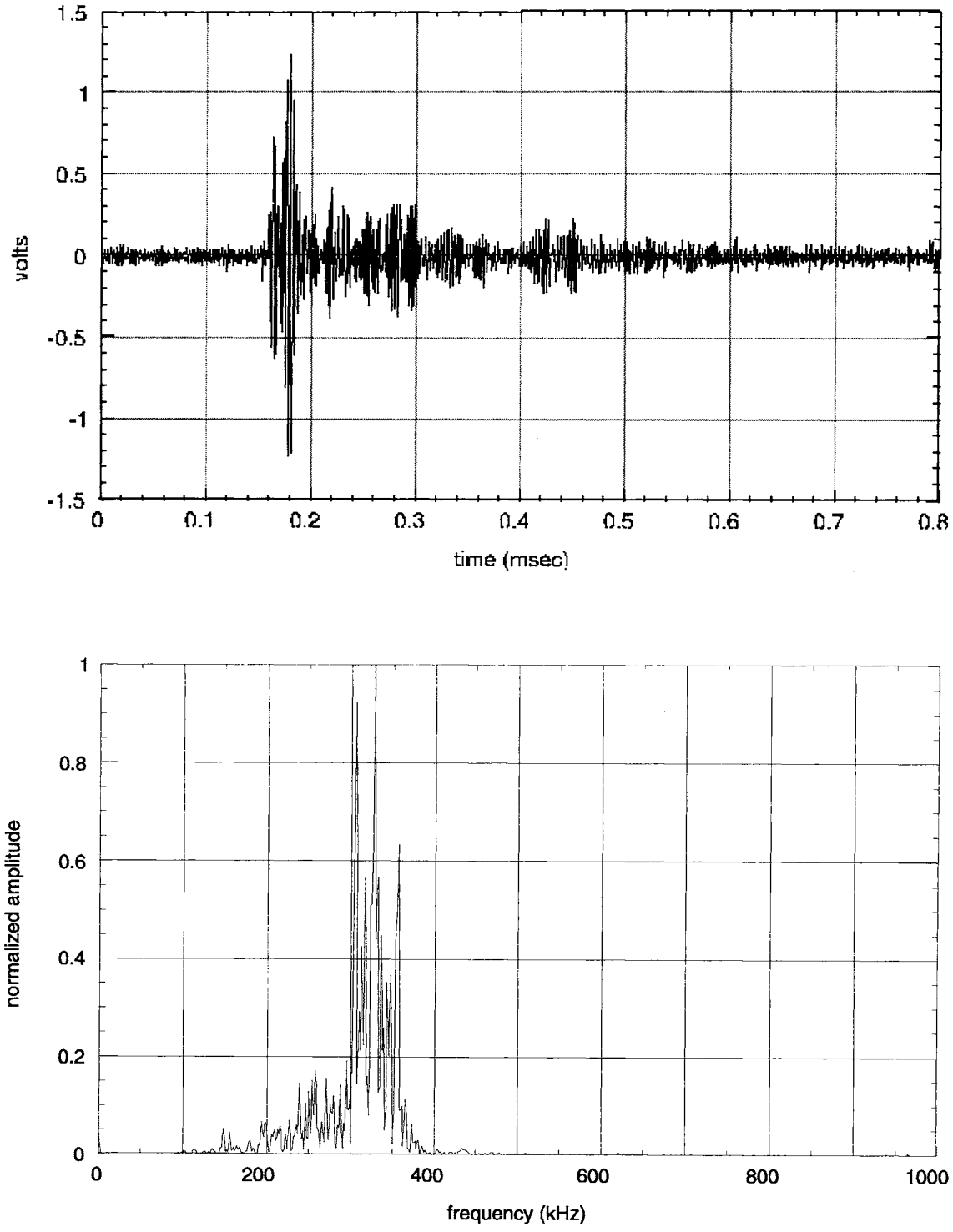

Figure 32. Typical noise waveform and its frequency spectrum as detected by R30I sensor.

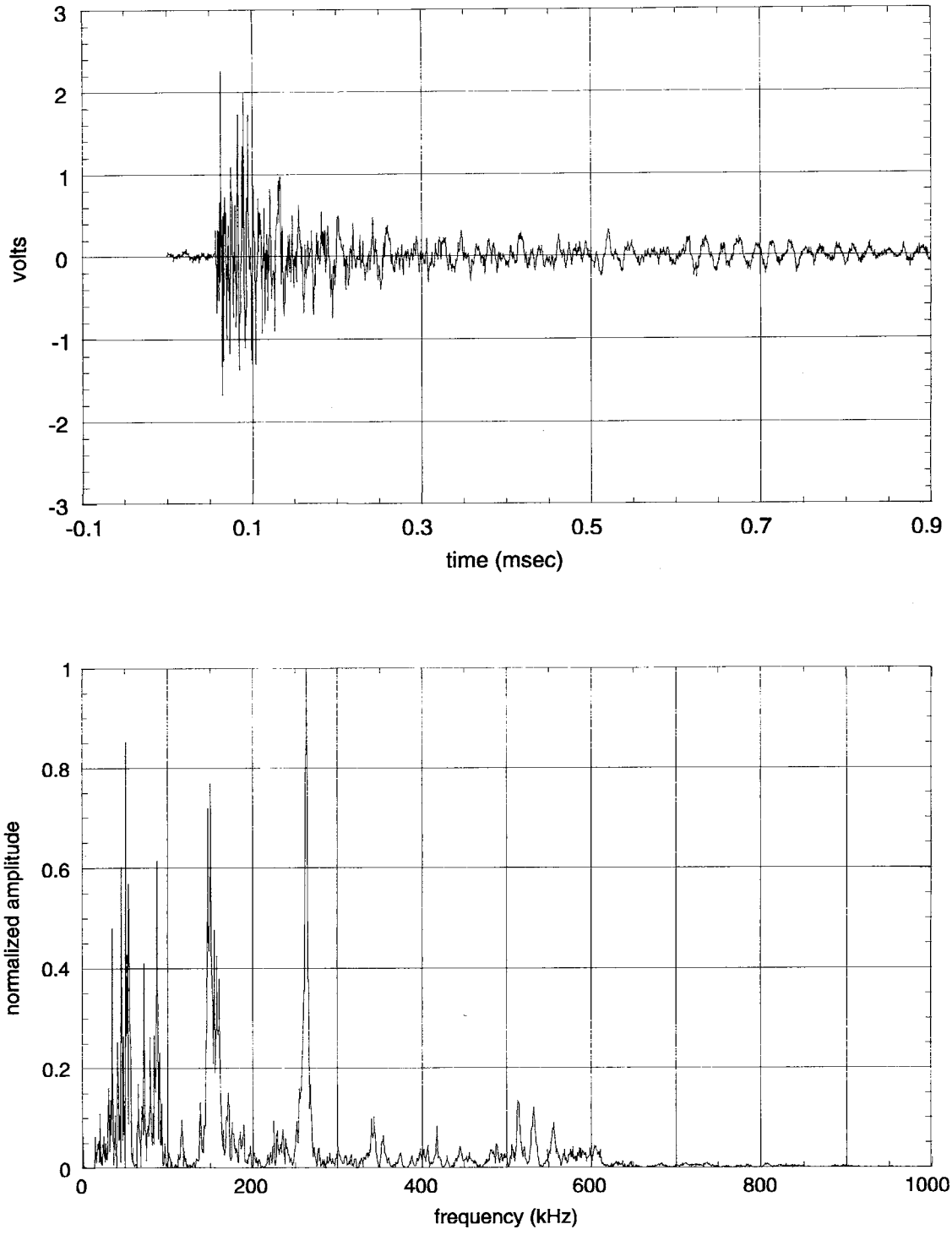

Figure 33. Wideband (WD) sensor waveform and normalized FFT of crack-related AE from crack #2.

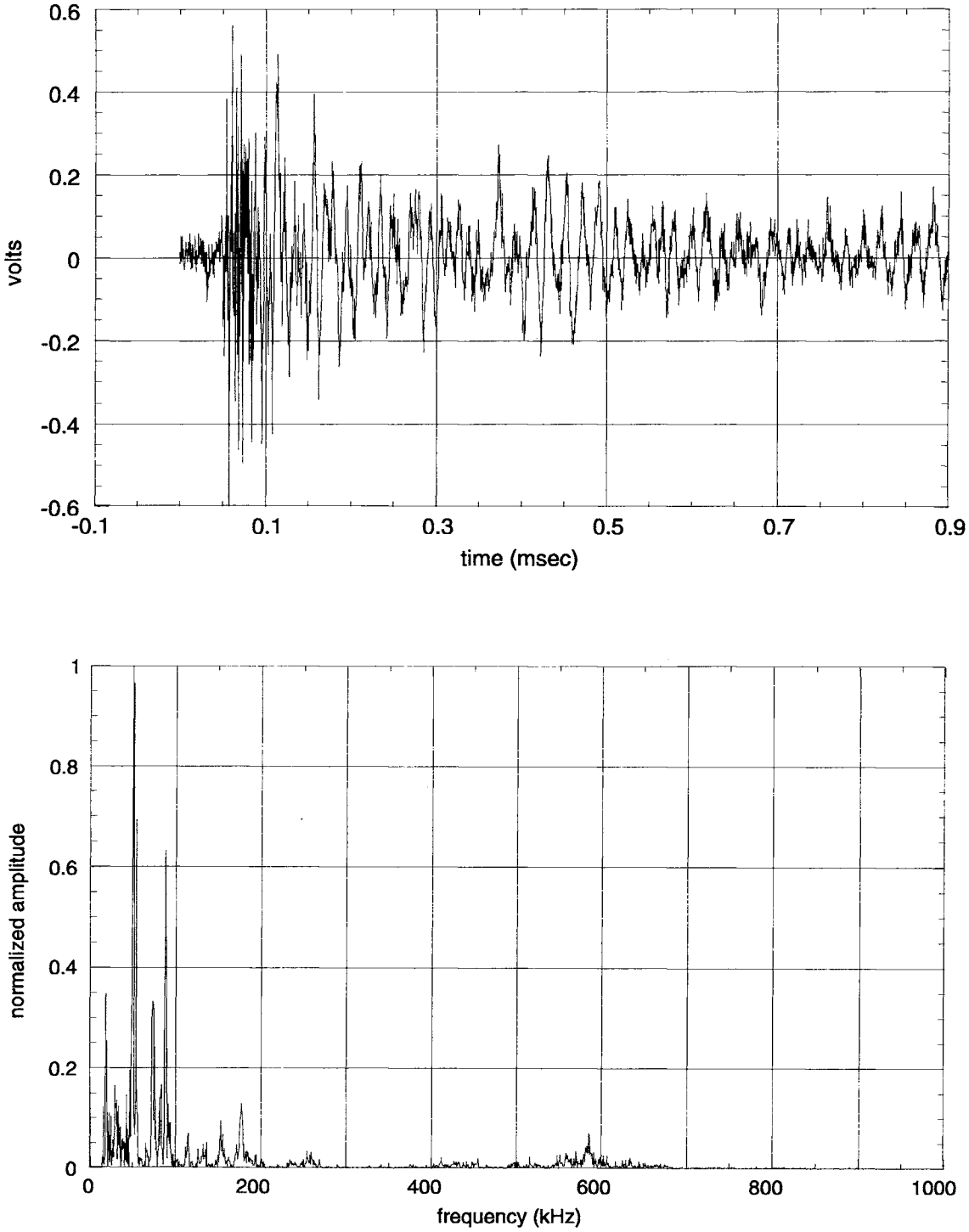

Figure 34. Noise waveform from crack #2 as detected by WD sensor.

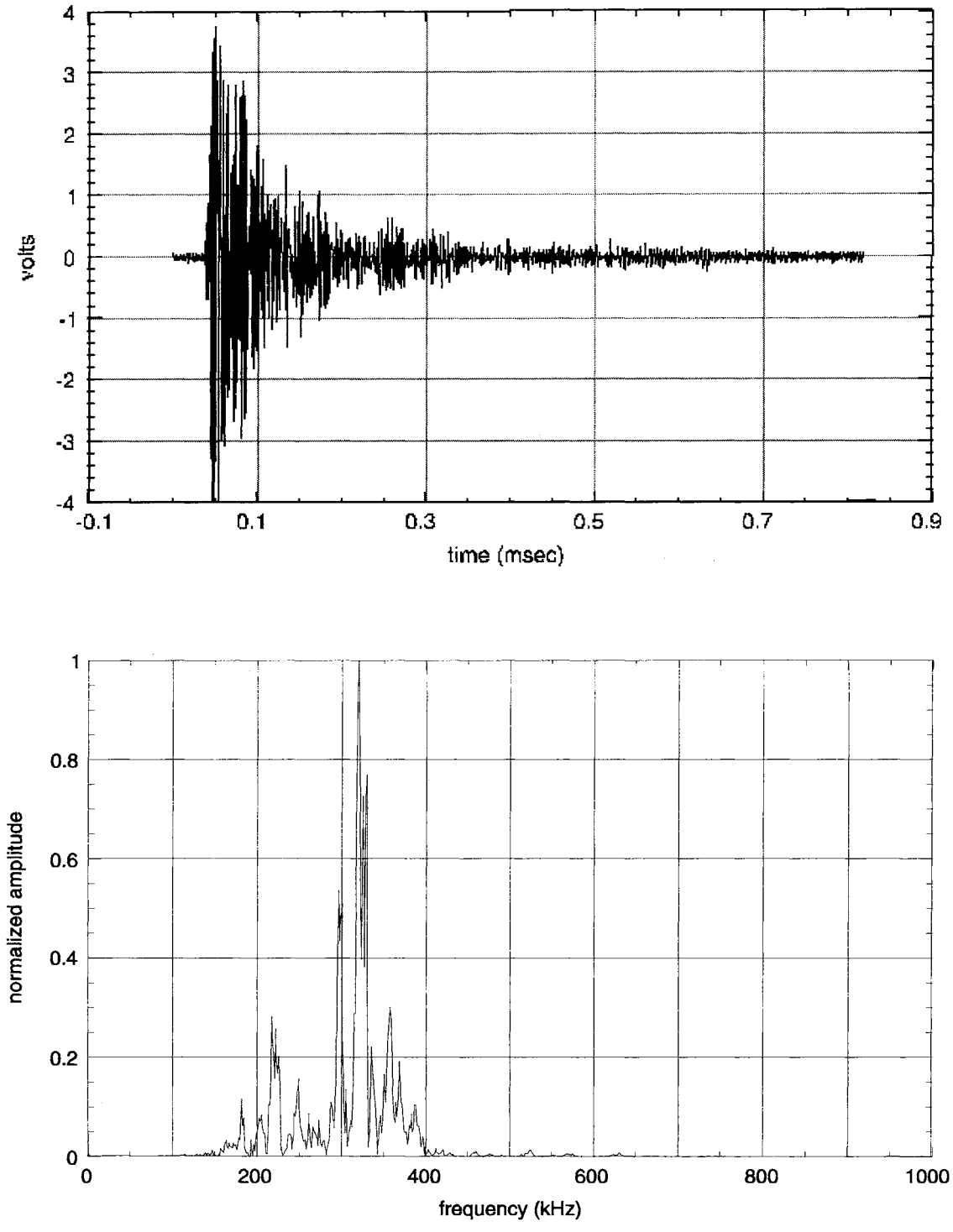

Figure 35. Resonant (R30I) sensor waveform and normalized FFT of crack-related AE from crack #2.

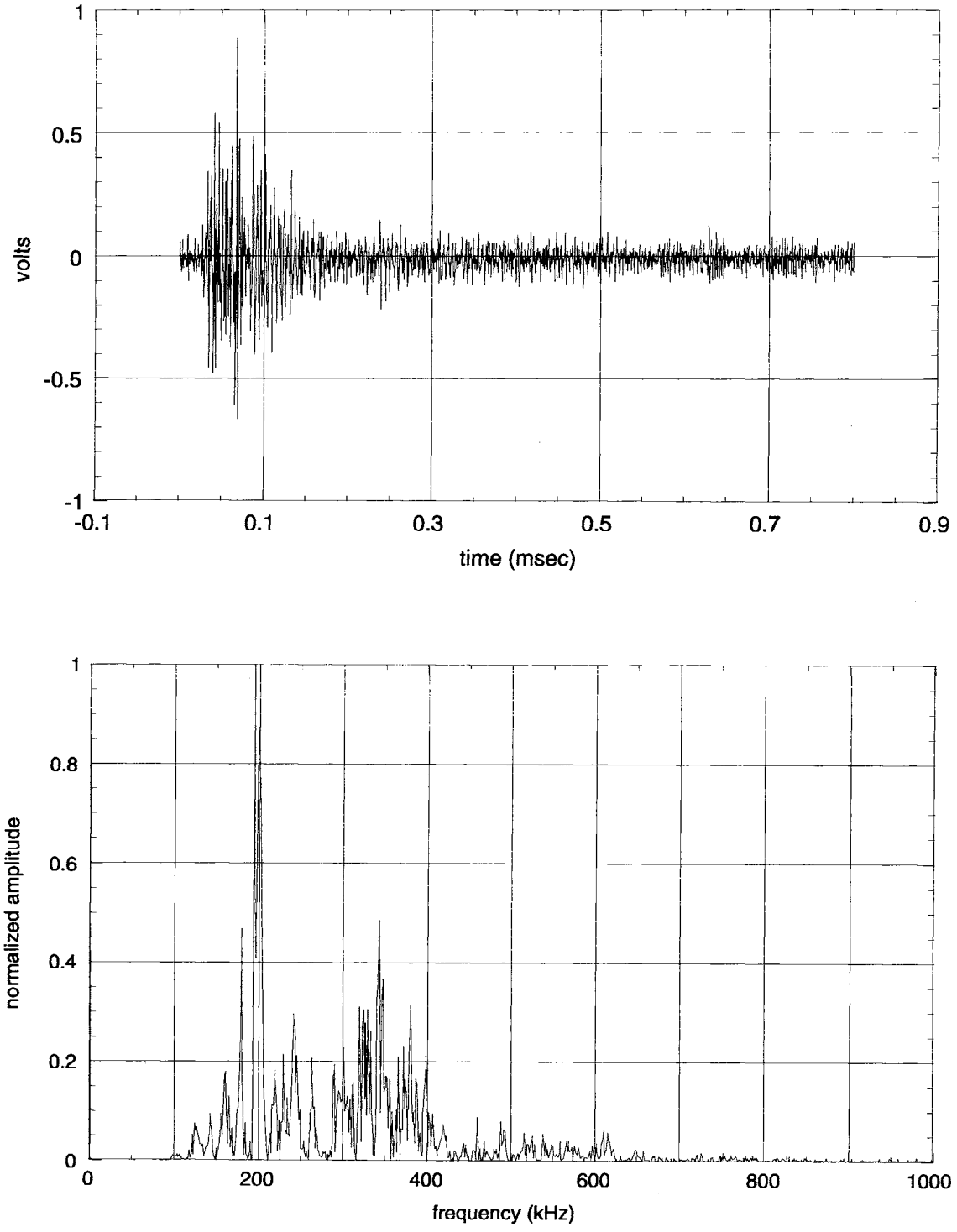

Figure 36. Noise waveform from crack #2 and its frequency spectrum as detected by R30I sensor.

Crack face rubbing signals are probably a significant portion of the detected crack-related AE. These signals have short risetimes and broad frequency content resembling AE produced by flaw-growth. The job of discriminating between the two types of signals is somewhat involved. Continuing work on the project includes further analysis of the waveforms collected from crack #2 to identify features to distinguish crack-growth signals from crack face rubbing. The strain gauge data will aid in this analysis.

The frequency characteristics of a detected AE signal depend on several factors, including source mechanism, transducer properties, part geometry and distance from source to sensor. The first and last of these may be responsible for the frequency profile of waveforms detected from crack #2.

Mechanical noise has frequencies distinctly lower than AE from the growth of a defect in steel. Fretting and rubbing noise, however, can have frequency spectra difficult to distinguish from crack AE. In the case of crack #1, source-to-sensor distance might influence the signals enough to differentiate between the two sources. Fretting noise that starts out with broadband frequency content may have its higher frequencies attenuated as it propagates along the material. This may explain why waveforms from outside the sensor 3 and 4 array monitoring crack #1 have lower peak frequencies than those originating from the crack. In the case of a crack well separated from noise sources, signal discrimination can classify crack and noise signals without the need for spatial discrimination.

The work of Vannoy et al.[11] on A-588 steel showed that the frequencies of crack AE tended to decrease as fatigue cycles and crack length increased. This suggests that the signals from crack #2 would have lower peak frequencies than those from the shorter crack #1. This must be considered as the classification of the waveforms from crack #2 continues.

A goal of the project was to determine the most appropriate type of sensor for bridge monitoring. Most previous studies of bridge monitoring used resonant sensors mainly for source location,[4,5,7,9,10,11,13-15] and wideband sensors only when frequency analysis was desired.[10,11] By using narrow band resonant transducers, the basic differences in the main frequency contents of noise and crack-related AE can be used to filter out irrelevant signals. Proper selection of sensor resonant frequency avoids the detection of lower frequency noise signals. However, this type of sensor, as mentioned earlier, tends to distort the features and intrinsic differences between AE signals more than wideband sensors do. This was pointed out by Miller et al.[8] who developed a field-worthy point-contact wideband sensor specifically for monitoring bridges.

The differences in the frequency content of noise and defect signals from crack #1 are very evident. Differences are also apparent in the AE time domain parameters. Using the range of values for counts, risetime, duration, energy and peak amplitude of the 12 flaw signals from crack #1 that were detected by the wideband sensor during the Oct. 25 test, filters were set up through which the noise signals were passed. A total of 930 noise signals were recorded from the wideband sensor, all of which were successfully filtered out. The same procedure was done

with crack AE and noise time domain data from the R30I sensor. Of the 201 noise signals collected, 162 were filtered out, an 80.6% success rate. Clearly, even without signal analysis, time domain data from a wideband sensor can classify crack-related emissions and noise better than data collected by a resonant sensor.

Load Discrimination

Figure 37 shows the strain levels on the hanger as vehicles crossed the bridge. Typically, the strain dips first before it sharply increases. This strain behavior may be assumed to be generally true at all points on the left side of the front surface of the hanger where crack #2 is located. In the presence of bending loads, the strain-time profile at the right side of the hanger can be considerably different. In this case, the recorded strain data could not be used to analyze results from crack #1.

The Spartan system can record strain gage readings concurrently with each recorded AE signal, determining the strain levels at which each emission occurred. Figure 38 is the time plot of strain near crack #2 as a truck passed over the bridge. Each point plotted on the line is an AE event. The graph shows that AE activity was detected at both high and low strain levels. Entire waveforms of most of these AE signals were recorded. This graph also plots the location of each of these events along the 1.2 m (4 ft) distance from sensor 6 to 2. No clear correlation appears between load levels and the location of the events.

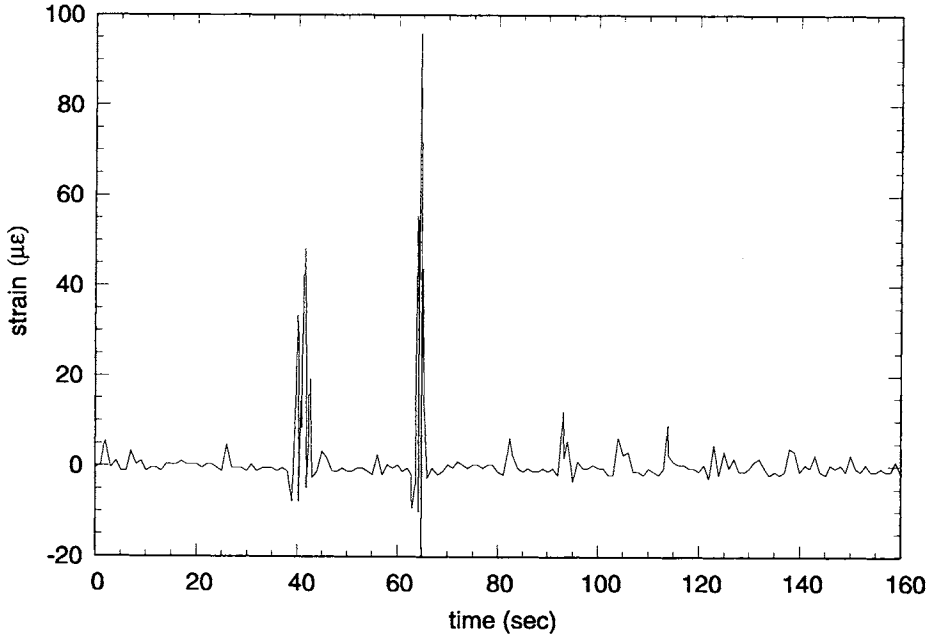

Figure 37. Typical plot of strain gage output versus time showing two major AE-producing events and numerous light load events.

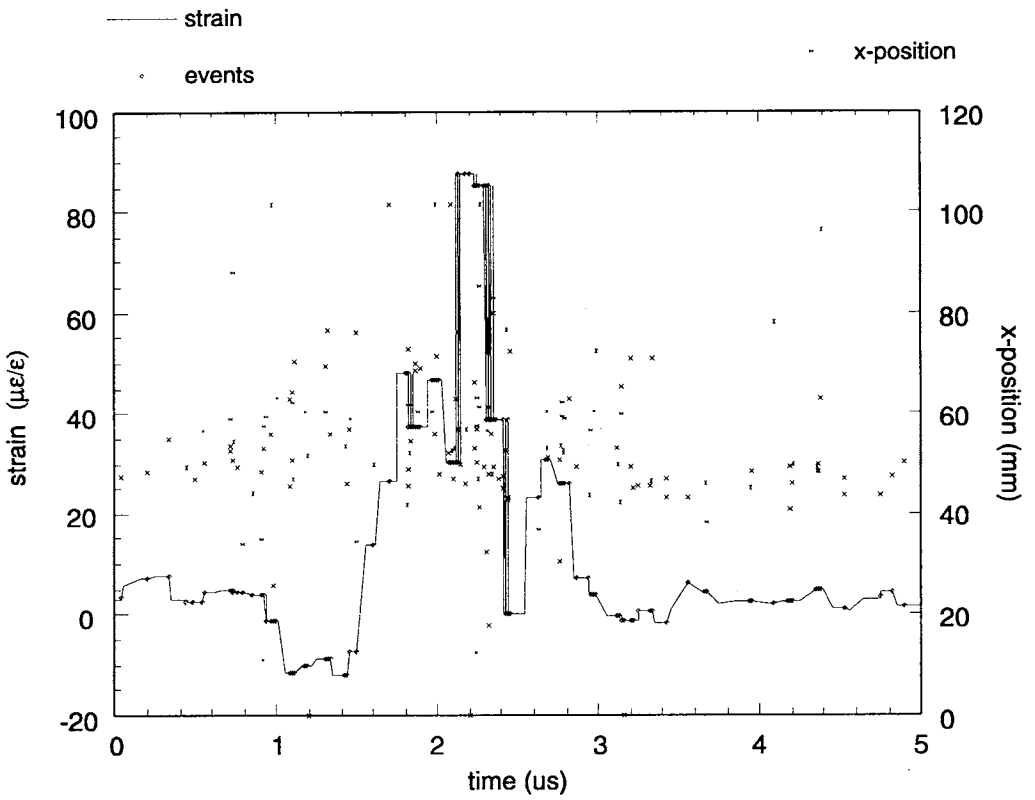

Figure 38. Time plot of strain near crack #2 as a truck passed over the bridge.

Correlating the available strain, location and waveform information for each AE event should reveal distinctive features that classify the AE events into 3 groups: fretting noise, crack face rubbing, and crack extension. Spatial discrimination techniques have effectively eliminated fretting noise as a concern. The challenge lies in distinguishing between rubbing and crack growth AE. If certain time and frequency domain features of AE signals correlated well with strain data, these features could distinguish events occurring at high strains from those produced at lower strains.

Summary Of Acoustic Emission Bridge Tests

Bridge	Detail	Problem	AE Test Results
Rte. 460 New River, Glenlyn, VA	Pin and hanger	Ultrasonically-detected crack on pin	No crack activity
Rte. 29 Staunton River, Altavista, VA	Girder web	a) Web crack; retrofitted with splice plate b) Web crack: arrested using stop drill holes	No crack activity
Rte. 671 Moormans River, Albemarle County, VA	Diagonal counter	Visible transverse crack on diagonal counter	No crack activity
I-66 south exit over Rte. 29, Gainesville, VA	a) Coverplate weld b) Lower web-to-flange weld	New repair welds	No crack activity
Rte. 29 Robinson River, Madison County, VA	Pin and hanger	4 visible cracks on 2 hangers	Crack activity detected from 3 cracks

CONCLUSIONS

1. Source location is highly effective for filtering noise sources that are spatially distinct and separable from monitored flaws. Guard sensors are necessary when noise activity outside the zone being monitored is high.

2. Crack activity is not constant. During 2 days of monitoring on the west hanger of the Robinson River bridge, detected AE shifted from crack #1 to crack #3. AE monitoring needs more time than the half-day periods in this study, especially when no activity is detected from a visible flaw.

3. The peak frequency of an AE signal is a powerful classifier that can distinguish between noise and crack-related emissions. In crack #1 of the Robinson River bridge, crack-related AE had peak frequencies of 275 KHz while noise signals peaked no higher than 200 KHz and were mostly less than 100 KHz.

4. Wideband sensors distinguish between crack-related acoustic emission and noise better than resonant sensors using either time-domain or frequency-domain parameters.

5. Filters using time-domain signal characteristics can be set up to eliminate the majority of noise signals.

6. Acoustic emission from cracks on bridge members can be detected throughout a load cycle and is not limited to positive live load levels. This is attributed to the detection of emission from crack face rubbing at the lower loads.

7. More study is needed to distinguish between crack growth and crack face rubbing signals. This will require waveform classification, frequency analysis and correlating AE, source location and strain data.

RECOMMENDATIONS

1. VDOT should develop a database on structures for the long-term AE monitoring of fracture-critical members suspected of containing cracks.

2. VDOT should integrate the real-time AE monitoring of bridge member deterioration into the bridge management/decision-making process at the federal and state level, in lieu of frequent visual inspections.

3. VDOT should train bridge inspection personnel in the installation and use of AE monitoring equipment.

ACKNOWLEDGMENTS

The authors thank D. B. Sprinkel and R. Truxell of the Culpeper District, W. L. Sellars of the Lynchburg District, and J. W. Lillard of the Northern Virginia District of VDOT for their cooperation and assistance; A. R. Zadeh of VPI & SU and C. Apusen and A. French of the Research Council for their technical support; and R. Combs and E. Deasy for their assistance with the graphics and photographs. C. Napier of the Federal Highway Administration, E. G. Henneke II of VPI & SU, R. Truxell of the Culpeper District, and M. M. Sprinkel of the Research Council reviewed the report and suggested helpful improvements. G. Mawyer edited the report. In addition, the authors express their gratitude to G. R. Allen for his continuous support of advanced NDE research at the Research Council.

REFERENCES

1. Pollock, A. A., and Smith, B. 1972. Stress-wave emission monitoring of a military bridge. *Nondestructive Testing*, 30: 348-353.

2. Argonne National Laboratory. *Formal proposal for acoustic emission of steel highway bridges*. Submitted to the National Science Foundation, April 1973.

3. Hopwood, T. 1976. *Acoustic emission, fatigue, and crack propagation.* Report No. 457. Kentucky Bureau of Highways.

4. Hutton, P. H., and Skorpik, J. R. 1975. *Acoustic emission method for flaw detection in steel for highway bridges.* Report No. FHWA-RD-78-97. Richland, WA: Battelle Pacific Northwest.

5. Hutton, P. H., and Skorpik, J. R. 1978. *Acoustic emission method for flaw detection in steel for highway bridges.* Report No. FHWA-RD-78-98. Richland, WA: Battelle Pacific Northwest.

6. Miller, R. K. (ed.). 1987. *ASNT nondestructive testing handbook*, vol. 5, p 330. ASNT, Inc.

7. Hartman, W. F. 1983. *Acoustic emission monitoring of electroslag and butt welds on Dunbar Bridge, West Virginia.* Report No. FHWA-WV-83-001. San Juan Capistrano, CA: Dunegan Corporation.

8. Miller, R. K., Ringermacher, H. I., Williams, R. S., and Zwicke, P. E. 1983. *Characterization of acoustic emission signals.* Report No. R83-996043-2. Hartford, CT: United Technologies Research Center, East.

9. Prine, D. W., and Hopwood, T. 1985. *Improved structural monitoring with acoustic emission pattern recognition.* Proceedings of the 14th Symposium on Nondestructive Evaluation, Southwest Research Institute, San Antonio, TX.

10. Vannoy, D. W., Azmi, M., and Liu, J. 1987. *Acoustic emission monitoring of the Woodrow Wilson Bridge*. Report No. FHWA-MD-87-06. College Park, MD: University of Maryland.

11. Vannoy, D. W., and Azmi, M. 1991. *Acoustic emission detection and monitoring of highway bridge components*. Report No. FHWA-MD-89-10. College Park, MD: University of Maryland.

12. Hariri, R. 1990. *Acoustic emission investigation and signal discrimination in steel highway bridge applications.* Ph.D. Dissertation. University of Maryland, College Park, MD.

13. Carlyle, J. H., and Ely, T. M. 1992. *Acoustic emission monitoring of the I-95 Woodrow Wilson Bridge*. Phase Report No. R90-259. Lawrenceville, NJ: Physical Acoustics Corporation.

14. Carlyle, J. H., and Leaird, J. D. 1992. *Acoustic emission monitoring of the I-80 Bryte Bend Bridge.* Phase Report No. R90-259. Lawrenceville, NJ: Physical Acoustics Corporation.

15. Carlyle, J. H. 1993. *Acoustic emission monitoring of the I-10 Mississippi River Bridge.* Phase Report No. R90-259. Lawrenceville, NJ: Physical Acoustics Corporation.

16. Gong, Z., Nyborg, E. O., and Oommen, G. 1992. Acoustic emission monitoring of steel railroad bridges. *Materials Evaluation*, 50, 883-887.

17. Prine, D. W. 1994. *Application of acoustic emission and strain gage monitoring to steel highway bridges.* Proceedings of the ASNT 1994 Spring Conference, New Orleans, Louisiana, March 1994, pp 90-92.

18. Fisher, J. W. 1984. *Fatigue and fracture in steel bridges: case studies.* p 37. John Wylie and Sons.

APPENDIX A

LABORATORY FATIGUE TESTING

At the beginning of the project, fatigue tests using compact tension specimens (CT) were done to characterize AE from A588 steel. The specimens, cut from 6.35 mm (0.25 in) thick plate, have the dimensions shown in Figure A-1.

EXPERIMENTAL PROCEDURE

An MTS 808 closed loop system with a maximum dynamic capacity of 20 kips was used in the tests. Loading was sinusoidal, tension-tension at frequencies of 0.25 cycles per second to 15 cycles per second. AE was measured at loading rates of 0.25 and 1.0 cycle per second. Data were acquired at every 1.6 mm (0.06 in) growth of the crack.

Fatigue property data was not available for A588. The appropriate loads for the tests were determined by trial and error. This was found to be 6 kN maximum and 0.2 kN minimum for an expected life of 150,000 to 200,000 cycles. Only two CT specimens, excluding the one used for trial and error, were tested.

An R30I resonant transducer and a wideband WD transducer were used. A thin layer of vacuum grease couplant was applied between the sensor face and CT specimen surface to ensure good transmission of AE signals. The transducers were held to the specimens by clamps; 3.7 m (12 ft) RG58 shielded coaxial cables connected the sensors to the Spartan data acquisition unit.

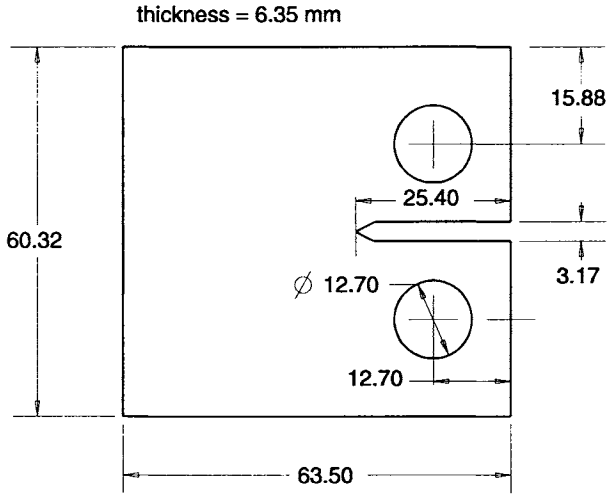

Figure A-1. Compact tension (CT) specimen.

The Spartan software, SA-LOC, was configured to record amplitude, ringdown counts, duration, risetime and energy. Load readings from the MTS machine were also recorded on the Spartan as parametric input #1.

Before proceeding with the actual tests, noise from the loading frame and grips was first determined so that system gains and thresholds could be adjusted to levels that would effectively ignore these noise signals. An R30I sensor was mounted on the lower hydraulic grip. With no test specimen installed, the grips on this head were engaged and the head was made to reciprocate while AE was measured and recorded. A CT specimen was then mounted and the two sensors attached to the specimen. While the proper loads were being determined by trial and error as explained earlier, AE activity from the trial specimen was also measured to determine the appropriate system sensitivity. A total system gain of 80 dB for both sensors and thresholds of 35 dB for the R30I sensor and 40 dB for the WD sensors was just high enough not to detect noise from the loading frame. Both sensor channels were set on floating mode so the data acquisition system would ignore high frequency hydraulic noise signals.

RESULTS

The relevant findings are shown in Figures A-2 to A-5. These are plots of amplitude, counts and energy against load. The first set, Figures A-2 and A-3, was taken after 53% of total fatigue life while the second, Figures A-4 and A-5, was recorded at 90.8% fatigue life. Both sets show two separate groups of AE events distinguished by the load levels at which they occurred. The cluster of events just above the minimum load are presumed to be caused by crack face rubbing. The high load events were produced by crack extension. Among the different AE parameters recorded, amplitude, counts and energy were the ones that highlighted the differences between the two groups of AE events.

Peak amplitude values and counts of rubbing signals are more scattered than those of crack signals. The higher counts of the rubbing signals were surprising. Since duration range is more or less the same for both groups, the higher counts may mean that rubbing signals have higher average frequency than crack-growth signals. Energy range, on the other hand, is more compact for the rubbing signals. The baseline of the energy plot also noticeably slants downward with decreasing load. This is most evident in Figure A-4.

Comparison of Figures A-2 and A-4 show that rubbing signals occur over a wider load range later in the fatigue life of the specimen. Probably a wider crack face area not only produces more rubbing, but also spreads out its occurrence over the load cycle.

The figures do not reveal the inconsistency in the appearance of rubbing signals. In some stages, mostly early and middle fatigue life, no rubbing signals were detected. Crack face rubbing may actually stop at certain times over the fatigue life of the specimen. This may be due to irregularities in the crack face which interfere more or less randomly.

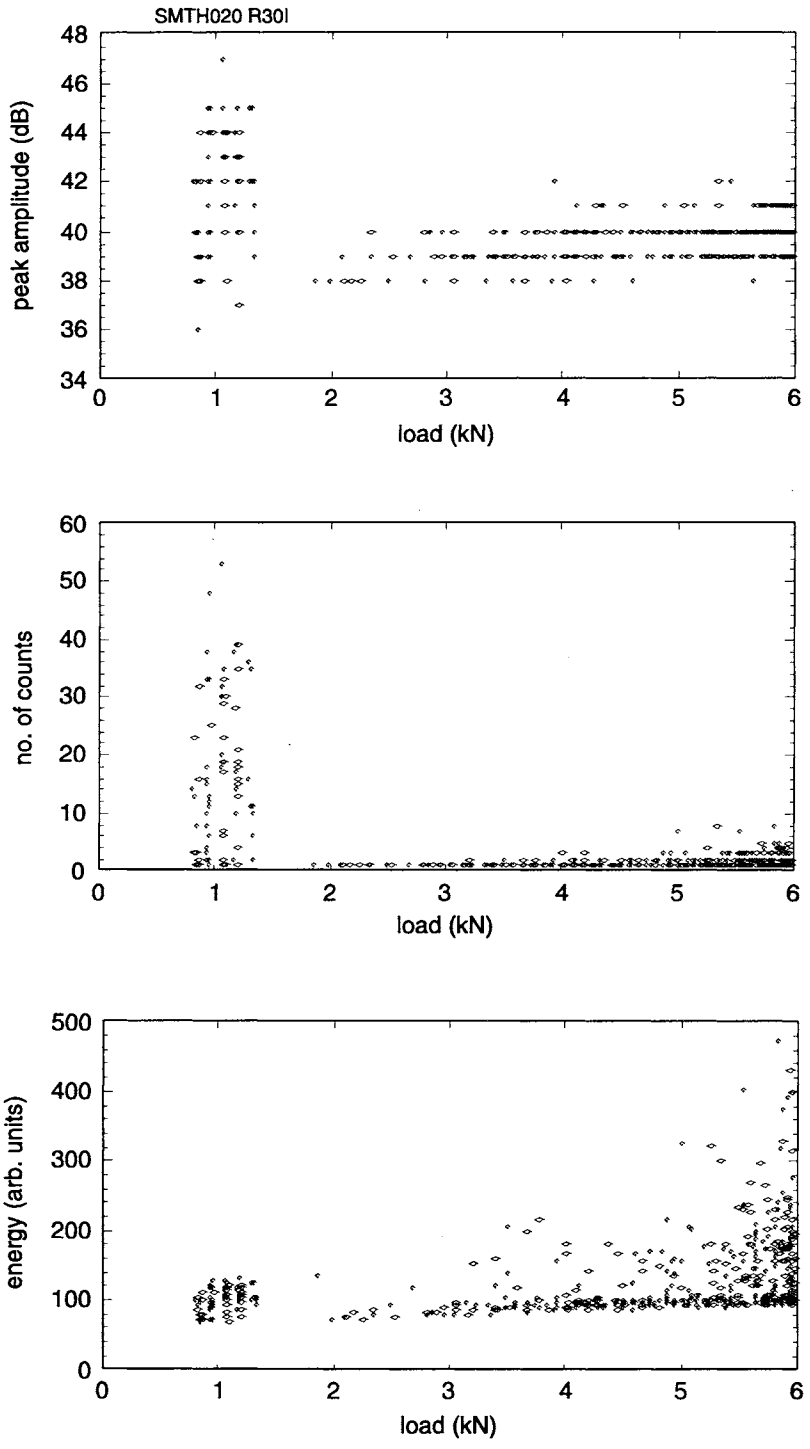

Figure A-2. Plots of AE parameters against load at 53% of fatigue life, R30I sensor.

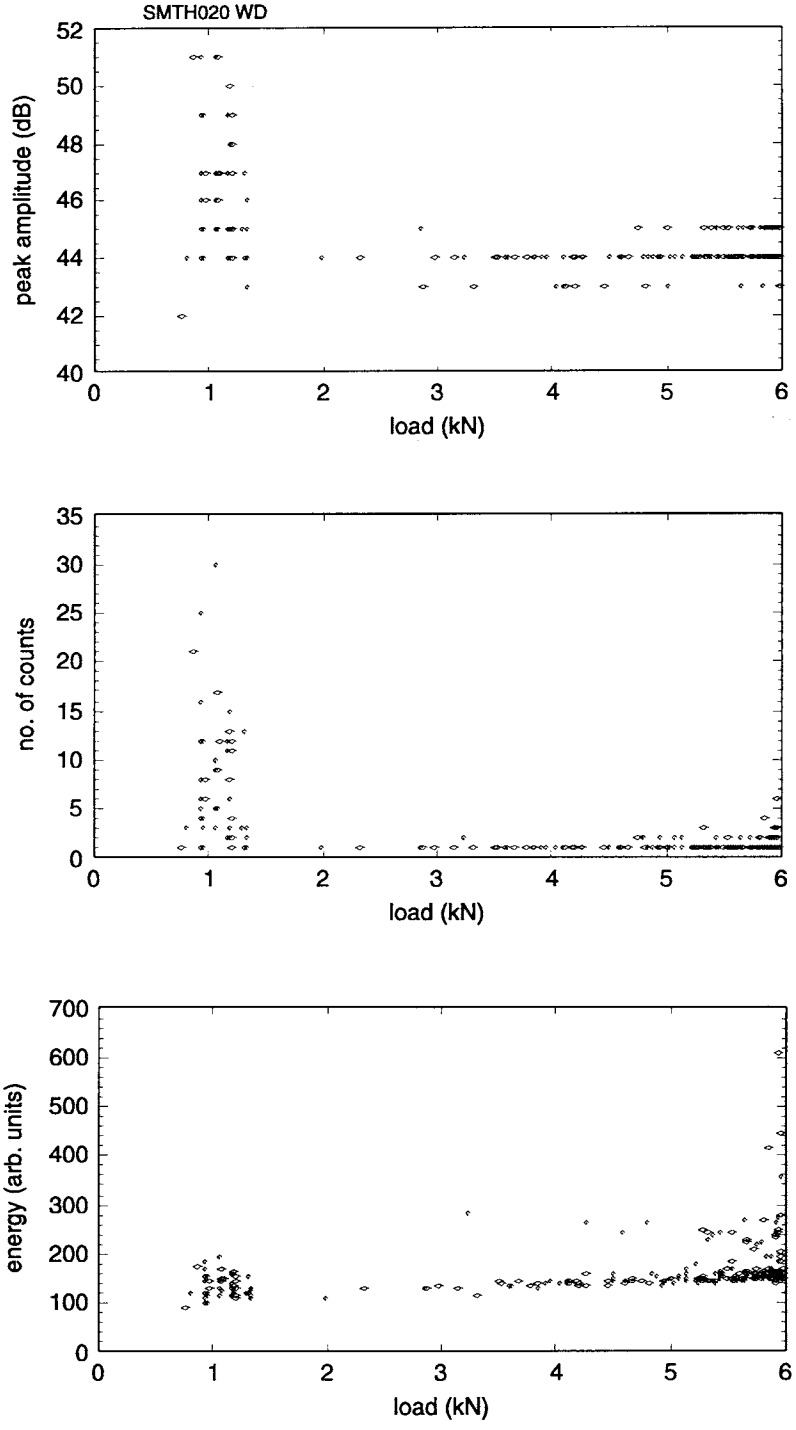

Figure A-3. Plots of AE parameters against load at 53% of fatigue life: WD wideband sensor.

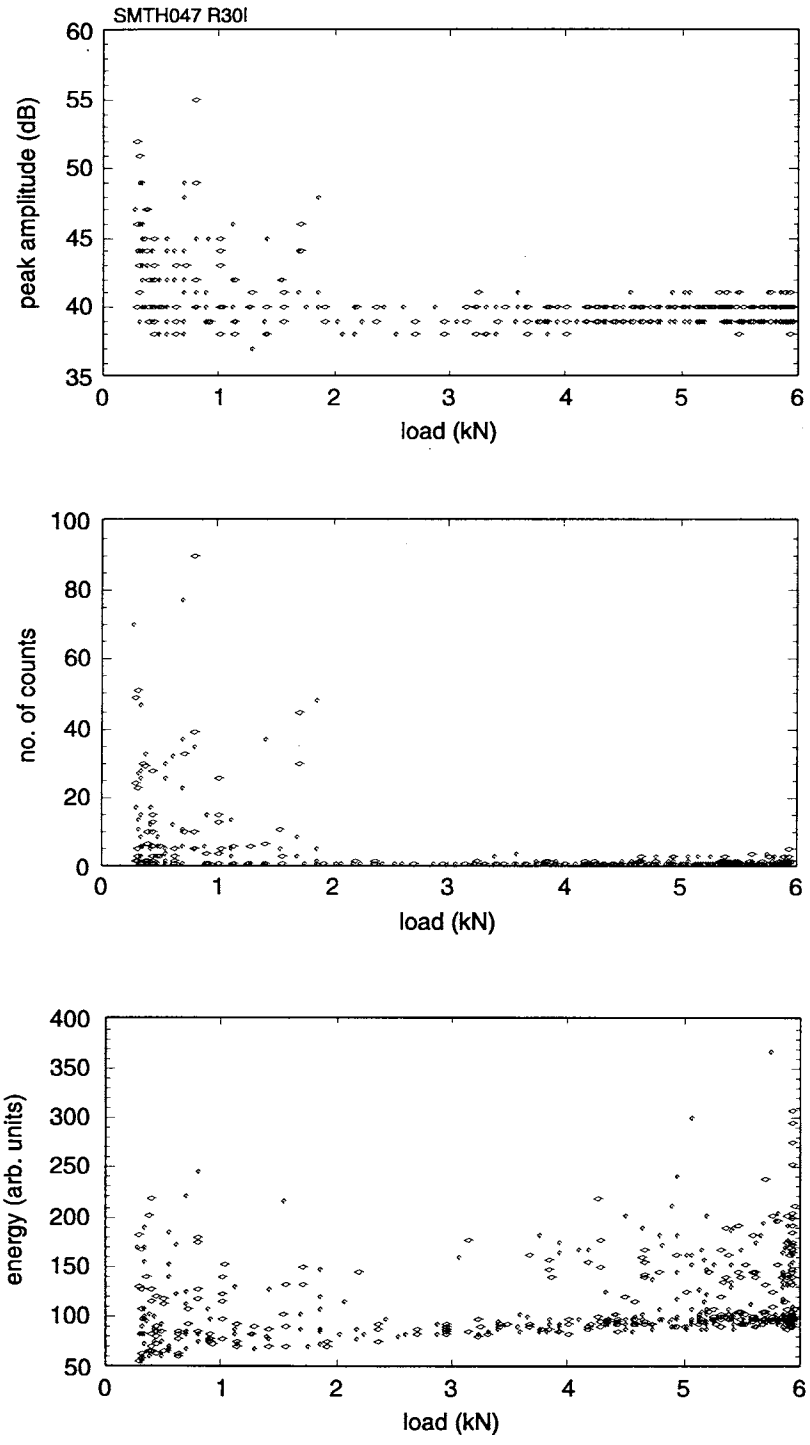

Figure A-4. Plots of AE parameters against load at 90.8% of fatigue life: R30I sensor.

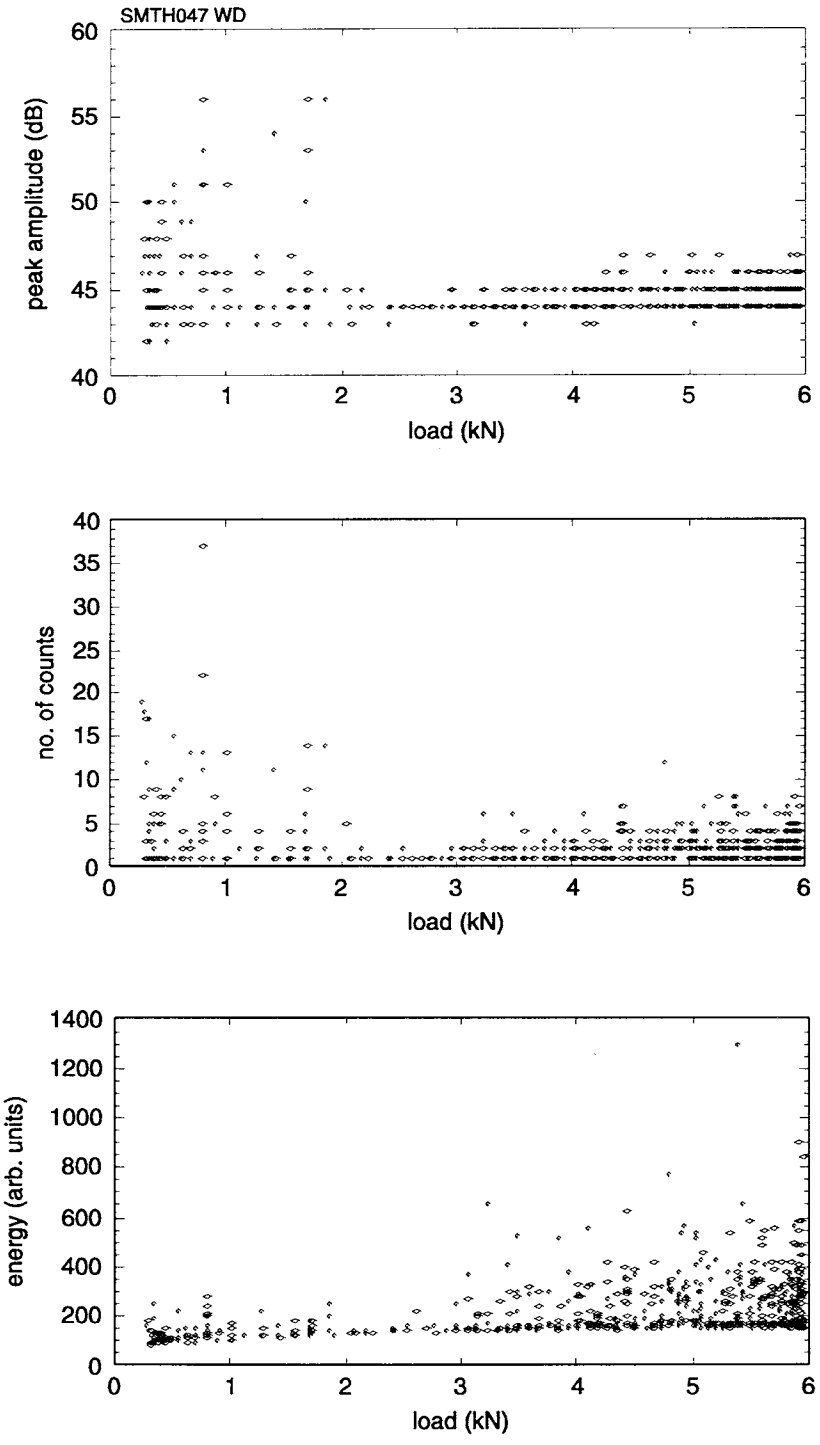

Figure A-5. Plots of AE parameters against load at 90.8% of fatigue life: WD wideband sensor.

Results from the R30I resonant sensor and the wideband sensor are generally the same. An exception is the energy parameter at the later fatigue stage. The energy of rubbing signals varies over a wider range for the resonant sensor, almost like the crack growth signals in Figure A-4. For the wideband sensor, the energy of rubbing signals remains bunched relative to the range of crack growth signals, as seen in Figure A-5.

Filters were developed using the range of all the measured AE parameters of crack extension signals for the earlier fatigue stage. Fifty-one out of 79 rubbing signals detected by the R30I sensor were filtered out, while only 36 out of 56 were eliminated from the WD data. Although not completely effective, these results show that parameter range filters can significantly reduce the number of detected rubbing signals. This could be useful in actual long-term monitoring, where any reduction in the amount of detected irrelevant data can significantly save computer memory or disk space.

APPENDIX B

TESTS OF TRANSDUCER MOUNTING ADHESIVES

In preparation for long-term AE monitoring on bridges, three adhesives were tested to assess their performance as bonding agents for transducer attachment. The three considered were hot-melt glue, five-minute epoxy and a cyanoacrylate adhesive. Hot melt glue has been used successfully on metal and fiberglass surfaces by the Monsanto Corporation (Saint Louis, MO), mainly to attach sensors for extended periods to pressure vessels which are periodically hydrotested. Five-minute Epoxy Gel, an epoxy resin manufactured by Devcon Corporation, is being used by Babcock and Wilcox Nondestructive Systems and Diagnostics Section personnel in their AE tests. Cyanoacrylate adhesive is a popular AE sensor bonding agent, ranking third in a survey conducted by ASTM in 1983.[1]

The same survey showed that the main cause of failure of bonding agents is differential expansion between the sensor and the specimen, induced either by strain in the specimen or by different thermal expansion rates. This was the main issue studied in the tests described below.

EQUIPMENT

Transducers

Six Model AC375L resonant transducers manufactured by Acoustic Emission Technology, with a nominal resonant frequency of 375 KHz.

Preamplifier

Model 1220A preamplifier with a 100 to 300 KHz bandpass filter manufactured by PAC.

Pulser

AE-CAL 2 acoustic emission simulator manufactured by Physical Acoustics Corporation. Amplitude, rise time, decay time and frequency of the pulse was user selected. The pulser itself was a V109 ultrasonic transducer manufactured by Panametrics, Inc.

EXPERIMENTAL PROCEDURE

The sensors were bonded to a 6 mm (0.25 ") thick piece of steel (Figure B-1) using different adhesives. The steel surface was sanded to remove dirt and was thoroughly cleaned before the sensors were mounted. Initial readings were taken with simulator settings of 10 s risetime, 10 s decay time, 300 KHz frequency and 80 and 70 dB amplitude at high dB setting. The sensor connection ports were taped over with masking tape to prevent ingress of moisture during exposure. The plate was then subjected to thermal cycling between the temperatures of 70F and 15F.

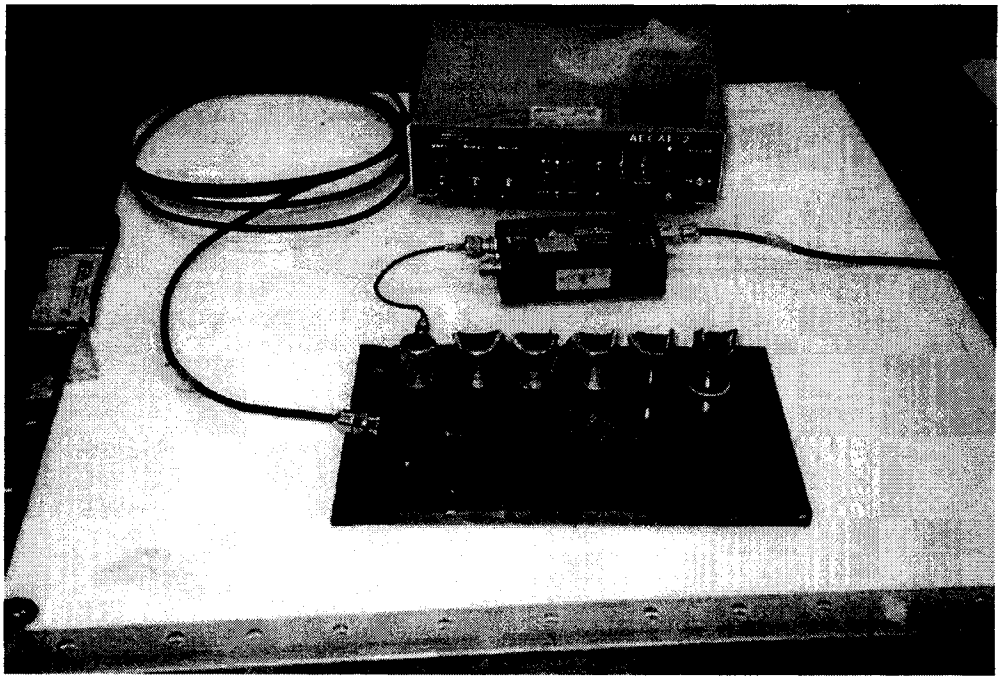

Figure B-1. Experimental set-up showing test plate, AET transducers, preamplifier and AE-CAL2 simulator.

RESULTS

Hot melt glue

Hot melt glue was difficult to use during the mounting of the sensors. The plate had to be heated so glue applied to the steel surface would not harden before the sensors could be bonded to it. Rigorous surface preparation was required for the bond to hold adequately. This adhesive was abandoned even before the plate was thermally cycled because bond strength was insufficient unless supplemented by a mounting instrument, such as a magnetic hold-down. Though practical for such applications as pressure vessels, a magnetic hold-down on a vibrating structure such as a bridge is not expected to perform well in the long term.

Five-minute Epoxy Gel

Three sensors were attached using 5-minute epoxy. The bonding agents were tested after 25 cycles by pulsing using the same AE simulator settings as in the initial test. One of the sensors detached after 20 cycles and another detached as the tape covering was being removed before the 25-cycle test. In both cases, debonding occurred at the sensor side. The remaining sensor was tested. The amplitude of the detected pulse was more than 10 dB lower than the initial reading. The use of this adhesive for long-term monitoring in an exposed environment is not recommended.

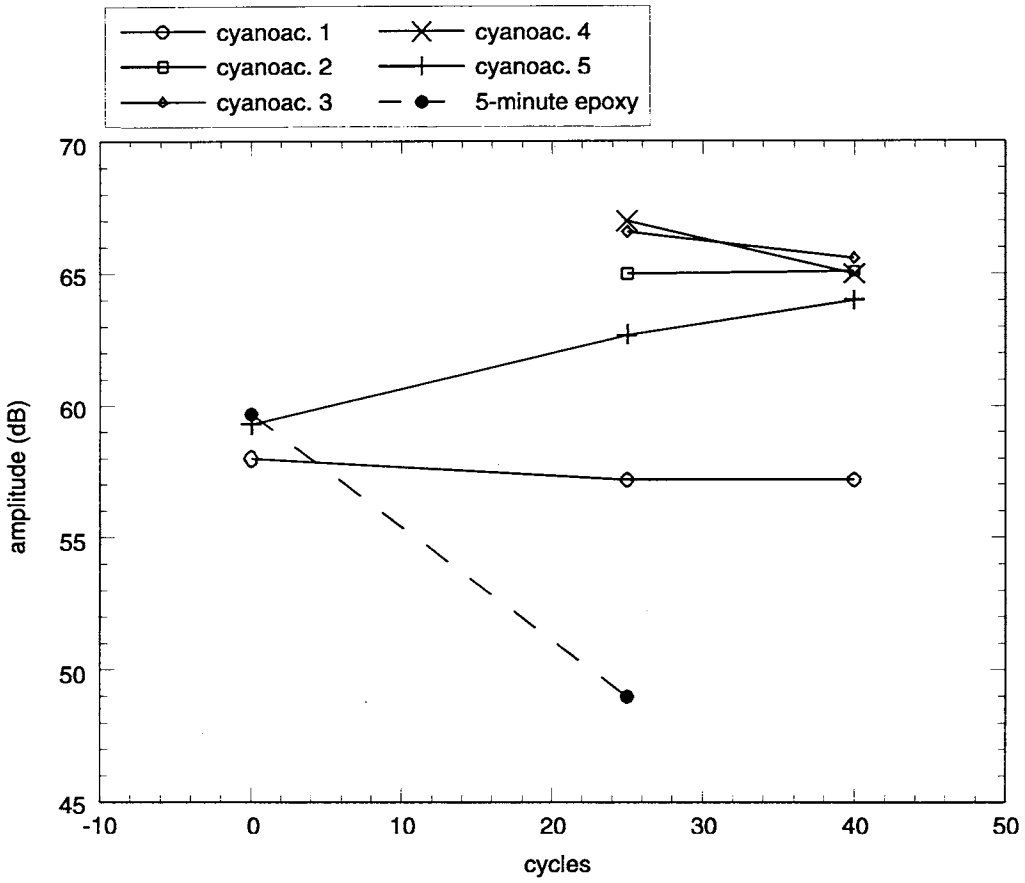

Figure B-2. Detected amplitudes of standard simulated AE signal from test sensors at 0, 25 and 40 thermal cycles.

Cyanoacrylate Adhesive

Initially, three sensors were attached using cyanoacrylate glue. After the failure of the five-minute epoxy, the two detached sensors were reattached using cyanoacrylate. Regular cyanoacrylate (True Bond super glue), which has a watery consistency, was used for the first three. Mounting was easier on the other 2 because a thicker, more viscous glue (Duro Quick Gel, Loctite Corporation) was used. Amplitude results taken at 25 and 40 cycles are shown in Figure B-2. There was practically no deterioration in the signal. The decrease shown by sensor 3 might be due to experimental error. One of the three original sensors detached after 25 cycles while the masking tape was being removed. The cause appeared to be insufficient adhesive. The regular cyanoacrylate flowed out from under the sensor before the bond could set. The sensor was reattached using the viscous type adhesive.

CONCLUSION

Of the three bonding agents tested, the viscous type of cyanoacrylate adhesive performed best under temperature cycling and is recommended for long-term bridge monitoring.

This investigation involves further cycling of the plate with the sensors attached with cyanoacrylate adhesive. Higher cycling temperatures will also be used to determine the effect on the bond. The effect of vibration on the bond will also be explored.

REFERENCE

1. Beattie, A. G. 1983. Acoustic emission couplants I: The ASTM survey. *Journal of Acoustic Emission*, 2, 67-68.